Facies (2009) 55:345–373
DOI 10.1007/s10347-008-0175-z

ORIGINAL ARTICLE

Quaternary carbonate-rocky talus slope successions (Eastern Alps, Austria): sedimentary facies and facies architecture

Diethard Sanders · Marc Ostermann · Jan Kramers

Received: 16 July 2008 / Accepted: 4 December 2008 / Published online: 8 January 2009

Abstract Quaternary carbonate-lithic talus slope successions of the Eastern Alps record an overall correlation between prevalent sedimentary facies, depositional geometry, and geomorphic maturity of the slope. After exposure of high cliffs by deglaciation or rocksliding, a low-dipping immature talus dominated by unsorted rockfalls initially accumulates. With progressive talus buildup, slope segments of different dips develop. Concomitantly, prevalent depositional processes change to grain flows and sorted rockfalls in the proximal, steep-dipping (35°–30°) slope segment, while deposits of cohesive debris-flows, ephemeral fluid flows and larger rockfalls prevail in the distal, lower-dipping slope segment. In mature talus deposystems, the proximal slope succession overlies the lower-dipping package of the distal slope along a thin 'downlap interval'. Immediately after cliff exposure by deglaciation or rocksliding, talus may aggrade at rates of up to a few tens of meters per 1,000 years, but the accumulation rate slows strongly with progressive maturity of slopes.

Keywords Eastern Alps · Quaternary · Talus slopes · Talus rocks · Facies architecture · Talus relicts

Electronic supplementary material The online version of this article (doi:10.1007/s10347-008-0175-z) contains supplementary material, which is available to authorized users.

D. Sanders (✉) · M. Ostermann
Institute of Geology and Palaeontology, University of Innsbruck, Innrain 52, 6020 Innsbruck, Austria
e-mail: Diethard.G.Sanders@uibk.ac.at

J. Kramers
Institute of Geological Sciences, University of Bern, 3012 Bern, Switzerland

Introduction

In the Northern Calcareous Alps (NCA, Fig. 1), relicts of Quaternary lithified talus-slope successions are common (Ampferer 1907), but to date were not subject to sedimentological inquiry. This is perplexing in view of the fact that the same successions triggered contrasting hypotheses on their palaeoclimatic and geomorphic significance (Ampferer 1907; Wehrli 1928; Cornelius 1941; Paschinger 1950; Van Husen 1981, 1983a,1983b, 1999). A talus slope is defined as an accumulation of "rock fragments of any size or shape (usually coarse and angular) derived from and lying at the base of a cliff or very steep, rocky slope" (Bates and Jackson 1980, p. 638). In the present Eastern Alps, post-Glacial talus slopes and alluvial fans are among the largest sediment bodies (Schrott et al. 2004). Investigations of talus slopes by reflection seismics or by ground-penetrating radar (Brückl et al. 1974; Sass and Wollny 2001; Schrott et al. 2004; Otto and Sass 2006; Sass 2006) mainly reveal total thickness, whereas corresponding sedimentary facies and facies architecture are rarely documented. It was often assumed that most, if not all, talus relicts accumulated and lithified during the Eemian. $^{234}U/^{230}Th$ disequilibrium dating of diagenetic cements, however, indicates that lithification of different talus slopes took place repeatedly during a documented interval from 480 ka to the Middle Holocene (Ostermann 2006).

In this paper, the sedimentary facies and architecture of Quaternary carbonate-rocky talus slope successions are described. Our results indicate that the facies architecture of talus successions developed in a predictable fashion with respect to prevalent facies, stratal dip, and depositional geometries. Whereas glacial-interglacial cycles determine the presence/absence of talus, as well as the altitude range of talus formation, minor climatic changes are difficult to

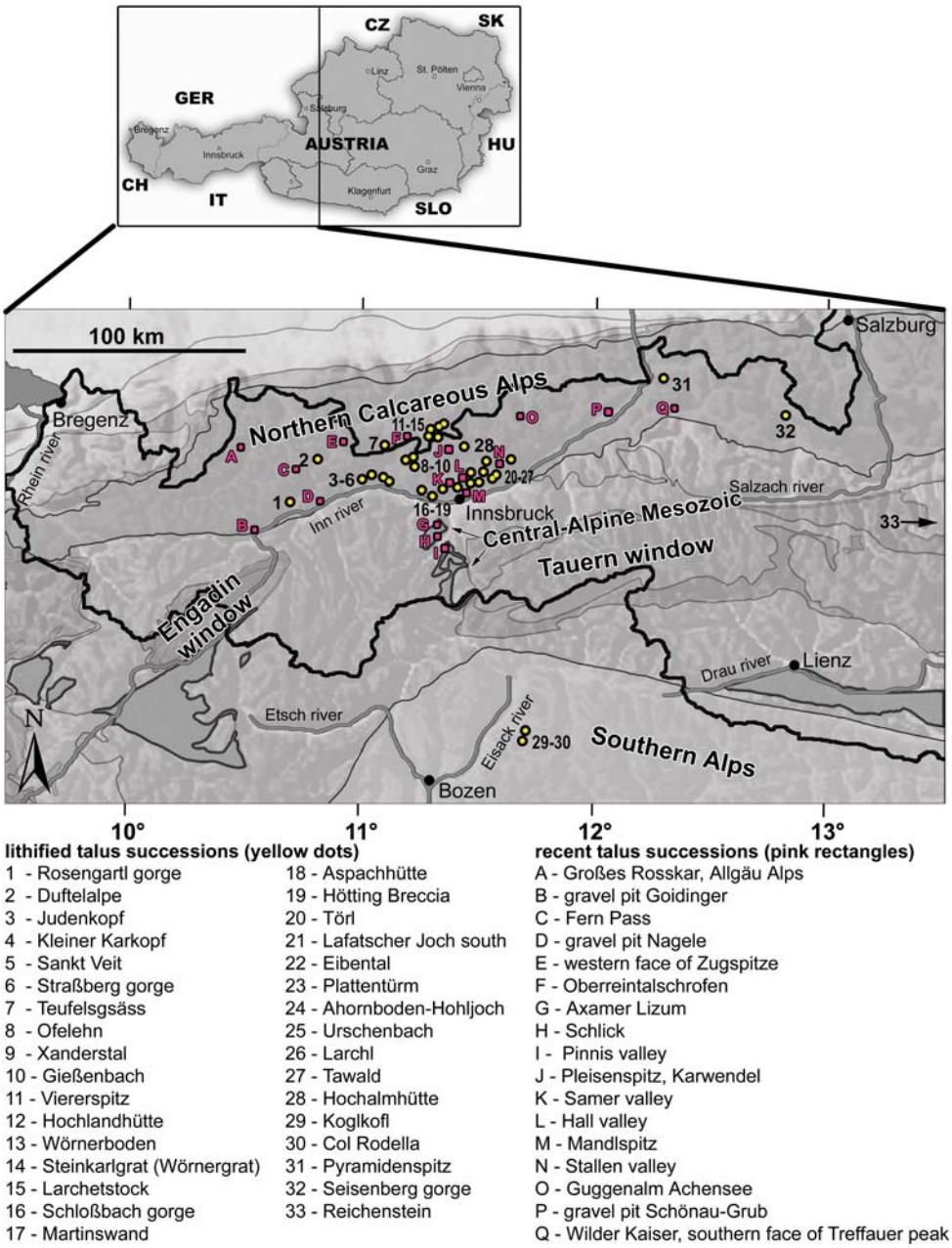

lithified talus successions (yellow dots)

1 - Rosengartl gorge
2 - Duftelalpe
3 - Judenkopf
4 - Kleiner Karkopf
5 - Sankt Veit
6 - Straßberg gorge
7 - Teufelsgsäss
8 - Ofelehn
9 - Xanderstal
10 - Gießenbach
11 - Vierer spitz
12 - Hochlandhütte
13 - Wörnerboden
14 - Steinkarlgrat (Wörnergrat)
15 - Larchetstock
16 - Schloßbach gorge
17 - Martinswand
18 - Aspachhütte
19 - Hötting Breccia
20 - Törl
21 - Lafatscher Joch south
22 - Eibental
23 - Plattentürm
24 - Ahornboden-Hohljoch
25 - Urschenbach
26 - Larchl
27 - Tawald
28 - Hochalmhütte
29 - Koglkofl
30 - Col Rodella
31 - Pyramidenspitz
32 - Seisenberg gorge
33 - Reichenstein

recent talus successions (pink rectangles)

A - Großes Rosskar, Allgäu Alps
B - gravel pit Goidinger
C - Fern Pass
D - gravel pit Nagele
E - western face of Zugspitze
F - Oberreintalschrofen
G - Axamer Lizum
H - Schlick
I - Pinnis valley
J - Pleisenspitz, Karwendel
K - Samer valley
L - Hall valley
M - Mandlspitz
N - Stallen valley
O - Guggenalm Achensee
P - gravel pit Schönau-Grub
Q - Wilder Kaiser, southern face of Treffauer peak

Fig. 1 Overview map of western Eastern Alps. Position of the investigated lithified talus successions is indicated by *dots with numbers* (see table in Appendix supplementary material for characterization of successions). Positions of active talus slopes shown in the following figures farther below are indicated by *red dots labeled with letters*. The Northern Calcareous Alps comprise a stack of cover thrust nappes dominated by Triassic carbonate rocks. The Central-Alpine Mesozoic is a parautochthonous cover succession on metamorphic basement, and is dominated by Triassic metacarbonates

unequivocally read from fossil talus successions. The highly non-steady character of talus accumulation combined with transient phases of inactivity or erosion devaluates talus successions as faithful recorders of palaeoenvironmental change.

Database, methods, and definitions

Facies interpretation is based largely on observations over more than 10 years in the Eastern Alps on present-day unlithified talus slopes, combined with surveys (down to a scale of 1/2000) of isohypsed satellite orthophotographs provided free on the Internet by the governments of the federal states of Austria. A total of 33 lithified or partly lithified talus successions of different age have been investigated (Fig. 1). The talus successions are indicated in geological maps of the Geological Survey of Austria and/or have been mapped in the field by the authors on a scale of 1/10000 or 1/5000. Cut and polished rock slabs and a total of 128 thin sections provided documentation of facies and diagenesis. For the method of age determination of cement by $^{234}U/^{230}Th$ disequilibrium dating, see Ostermann et al. (2006, 2007). Definitions of technical terms of geomorphology and sedimentology can be viewed in the electronically supplemented material. According to the

scale subdivision of forms by Summerfield (1991, his Table 1.1), the features dealt with in the present paper pertain to eighth- to tenth-order forms (see Appendix in supplementary material). For easier communication, herein we designate eighth-order forms (1–10 km^2) as macro-scale, ninth-order forms (1 m^2 to 1 km^2) as meso-scale, and tenth-order forms (1 mm^2 to 1 m^2) as micro-scale.

Geological setting

The Eastern Alps are dominated by stacked thrust nappes of the Austroalpine tectonic unit (Fig. 1; Schmid et al. 2004). Most carbonate-lithic talus successions mentioned herein are situated in the NCA and in the 'Central-Alpine Mesozoic' (CAM) of the Upper Austroalpine unit (Fig. 1). The successions both of the NCA and the CAM are dominated by Triassic shallow-water carbonates (Table 1). The NCA formed during Late Jurassic, Early Cretaceous, and Paleogene phases of (accelerated) convergence and stacking of cover thrust nappes. The CAM, in contrast, rests parautochthonous on Austroalpine basement, and was overridden by the nappe stack of the NCA. The stratigraphic succession of the CAM is dominated by metadolostones (Table 1). During the Late Paleogene to Neogene, the Austroalpine nappe stack was subject to uplift and wrench faulting (Linzer et al. 1995). Uplift and erosional dissection started earlier in the western Eastern Alps, while the eastern part remained buried until a few Ma ago below a truncation surface ('Augenstein surface') veneered by fluvial deposits. Further uplift combined with Pleistocene glaciations nearly totally obliterated the Augenstein surface. The present scenery of the Eastern Alps was almost entirely shaped by glacial-interglacial cycles (Van Husen 1999; Frisch et al. 2000, 2001). Partly as a result of later uplift, the eastern sector of the NCA today is rich in plateau-like massifs, whereas the western NCA are characterized by roughly W to E-striking ranges with di- and tri-hedral summits (cf. Frisch et al. 2001).

Because of their intense tectonic deformation, the carbonate rocks of the NCA and CAM are prone to frost cracking and high rates of debris production (cf. André 1997). In the present NCA, the major volume of sediment is stored in alluvial fans and in talus slopes (Schrott et al. 2004). Commercial gravel pits and natural outcrops indicate that carbonate-rocky, post-Glacial talus successions are typically tens of meters up to about 100 m in thickness. For the Eastern Alps, observations in talus successions, and their relation to other Quaternary deposits, indicate significantly increased debris production by intensified physical weathering of rocky slopes shortly before and immediately after glaciations (Van Husen 1983b; Ostermann 2006;

Table 1 Main lithological units that nourish carbonate-rocky talus slopes (Eastern Alps), and some of their attributes relevant to talus formation

Name (age)	Main area of distribution Typical thickness range (in m)	Attributes relevant for talus production
Wetterstein Limestone (Ladinian to Lower Carnian)	Western NCA 500–1,000 m	Moderate to high weathering resistance. Weathers mainly into gravels to cobbles, scarce matrix
Wetterstein Dolomite (Ladinian to Lower Carnian). Dolomitized equivalent to Wetterstein Limestone	Eastern NCA 500–700 m	Low weathering resistance. Weathers easily into sand and gravels, matrix copious
Hauptdolomit unit (Norian)	Western NCA 1,000–1,500 m (up to >2,000 m)	Low weathering resistance. Weathers easily into sand and gravels, matrix copious
Dachstein Limestone (Norian to Rhaetian)	Eastern NCA 1,000–1,500 m (up to >2,000 m)	High weathering resistance. Weathers mainly into gravels to boulders, scarce matrix
Unterer Dolomit (Anisian *pro parte* to Lower Carnian). Equivalent to 'Alpine Muschelkalk' Auct. and to Wetterstein Limestone.	CAM south of Innsbruck 400 m	Metamorphic, no or little penetrative deformation Moderate weathering resistance. Weathers easily into sand and gravels, matrix copious
Oberer Dolomit (Norian). Equivalent to Hauptdolomit unit	CAM south of Innsbruck 500 m	Metamorphic, no or little penetrative deformation Moderate weathering resistance. Weathers easily into sand and gravels, matrix copious

All of the mentioned units accumulated from shallow-water carbonate platforms

NCA Northern Calcareous Alps, *CAM* Central Alpine Mesozoic

Sanders and Ostermann 2006). Today, depending on local conditions (lithology, slope aspect, jointing, etc.), most carbonate-lithic alluvial fans and talus slopes below about 1,800–1,400 m a.s.l. are of low activity or abandoned, more-or-less vegetated, and subject to linear erosion. Conversely, most talus slopes higher up are typically still in accumulation, but most probably at lower rates than immediately after deglaciation. The typical thickness of talus slope successions, combined with U/Th cementation ages of post-Glacial talus successions (Ostermann 2006), indicate that the talus slopes of the NCA formed at rates of roughly 10 m/ka to a few tens of meters per 1,000 years. Talus slopes that shed into detachment scars of age-dated rockslides in the NCA (cf. Patzelt and Poscher 1993; Ostermann et al. 2007; Prager et al. 2007) record similar aggradation rates. In the NCA, the preservation of lithified talus successions ranges from practically complete to erosional relicts a few tens of meters in size. In each sector of the lithified talus slopes, the amount and variability of bedding dip is in the same range as the surface dip of actual, unlithified talus (cf. Francou and Manté 1990). This indicates that no significant tectonic tilting of bedding took place. Similarly, in clast interstices of the lithified successions, geopetal fabrics of infiltrated mud to sand do not suggest substantial tilting.

Cliff/talus ensembles: general pattern of development

The rate of physical weathering of rock cliffs and talus production is mainly controlled by density of bedding, joints, faults, and (if present) schistosity. Thin-bedded and/or jointed and faulted carbonate rocks are highly susceptible to physical weathering, in particular to frost cracking (André 1997; Prick 1997). Talus slopes hence accumulate most rapidly in a wet-periglacial climatic/altitudinal 'talus window' with frequent freeze-thaw cycles (Fig. 2a) (Bertran and Texier 1994; Coltorti and Dramis 1995; André 1997; McCarroll et al. 2001; Hales and Roering 2005). Over glacial-interglacial cycles the 'talus window' (Hales and Roering 2005) varies considerably in altitude. Field observations (Penck 1924), degradation of man-made cliffs (Hutchinson 1998), and mathematical analyses (Bakker and Le Heux 1952; Caine 1969; Obanawa and Matsukura 2006) indicate that the onlap surface of an aggrading talus slope develops in a convex shape while the cliff retreats in its original steepness and declines in vertical height (Fig. 2b). The cliff is therefore progressively replaced by the convex onlap surface of the talus ('slope replacement', Summerfield 1991). Upon cliff degradation and retreat, a progressively smaller cliff area can produce talus. The rate of talus aggradation thus decays exponentially (Fig. 2c) (Hutchinson 1998; Obanawa and Matsukura 2006). During talus accumulation, the slope of its surface steepens from initially low-dipping to steep-dipping, until a stable dip value of a 'mature' talus slope is attained (Fig. 2d) (Kirkby and Statham 1975; Clowes and Comfort 1987). 'Talus maturity' is a dimensionless ratio of vertical height (H_t) of talus to vertical height (H_s) of the entire slope (Fig. 2d). For rockfall-dominated talus, a value $H_t/H_s \geq 0.4$ characterizes a mature slope (Statham 1976). When a mature slope configuration has been attained, the talus further aggrades by an upward shift of its surface at overall constant slope dip (Fig. 2b, increments t_3–t_5), until the cliff is degraded and talus aggradation is terminated.

Similar to marine shelves or rivers (Pitman and Golovchenko 1983; Morris and Williams 1999; Chorley 2000), the shape and dip of a talus slope is geomorphically graded to prevalent processes of sediment transport and deposition. Down slope along talus deposits, in many cases, different processes of sediment supply, transport, and deposition prevail in different slope segments (Fig. 2b). The proximal part of many active Alpine talus slopes is dominated by grain flow and rockfall. Conversely, in the distal part of slope, debris flows and ephemeral alluvial processes may prevail. As a result of slope grading to different prevalent processes and/or to different rates of sediment supply (cf. Allen 1970; Chandler 1973), talus slopes are characterized by segments of different dip separated along knick lines ('psi-points', Fig. 2b) (Francou and Manté 1990; see also Kotarba and Strömquist 1984). The number of knick lines on a talus slope depends mainly on prevalent processes; commonly one or two slope breaks are identified (Jomelli and Francou 2000). In lithified talus successions, the dip of a former slope surface is recorded by dip of bedding which, in turn, allows estimation of proximality even if the succession is incompletely preserved. Generally, on the majority of talus slopes, from proximal to distal mean grain size increases, while grain sorting and expression of bedding or stratification tend to decrease (Fig. 2b).

Present carbonate-rocky talus slopes, Eastern Alps

For a better understanding of facies and architecture of lithified talus, the main types of and controls on the present carbonate-rocky talus slopes of the Eastern Alps are briefly outlined below.

Mountain morphology

The western NCA are formed of steep-flanked mountain ranges with di- and tri-hedral summits. Comparatively small cirques were excavated by cirque glaciers, which today are nearly all absent. Cliffs commonly range up to

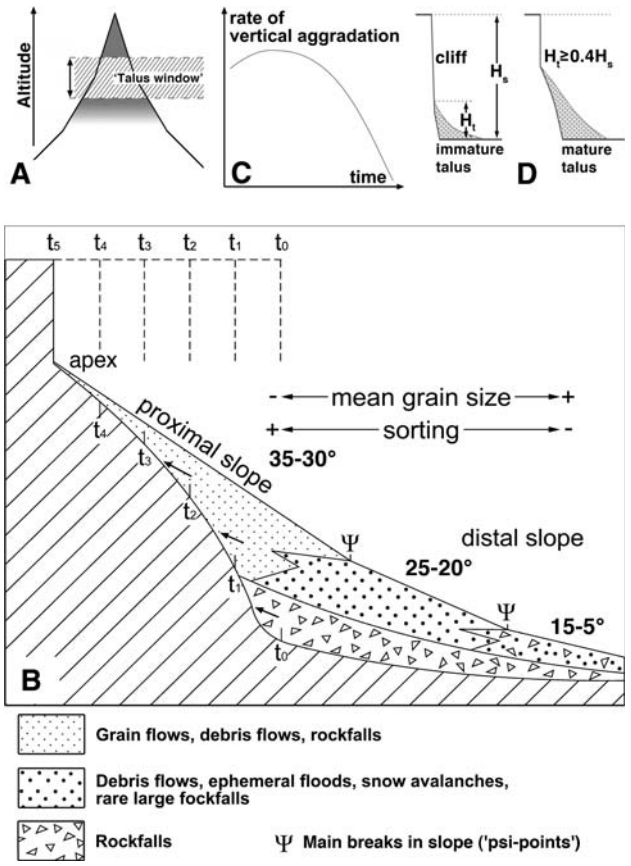

Fig. 2 General patterns of rock cliff/talus development. **a** Talus formation proceeds most effectively in an altitudinal/(micro-)climatic 'talus window' with numerous freeze-thaw cycles. **b** Cliff degradation and talus accumulation. *Dashed lines* t_0–t_5 indicate positions of rock cliff at different times. Initially, at time t_0, the cliff has maximum height: at this stage, a rockfall-dominated talus of low slope inclination accumulates. Later, upon progressive steepening of the talus slope, besides rockfalls, other processes such as debris flows and ephemeral floods gradually shape the surface and determine sedimentary facies. The onlap surface of the talus slope onto the retreated portions of the cliff develops with a convexity (see text). When the talus slope attained a stable configuration, its proximal segment steepened to 30°–35°. In this stable (mature) state, the talus aggrades while the dip of the onlap surface progressively approaches the angle of residual shear of the proximal talus slope, until a graded rocky slope develops. Because different processes of sediment transport and deposition prevail in different portions of the slope, mature talus slopes are divided into slope segments of different dip (slope knick lines = 'psi-points'). **c** Because the area of the retreating cliff becomes exponentially smaller, the rate of talus aggradation tends to diminish in an exponential fashion, too. **d** Immature talus slopes typically show a vertical height $H_t < 0.4$ of the vertical height H_s of the entire slope. Mature talus slopes are characterized by $H_t \geq 0.4H_s$

closely below or directly towards the summit (Fig. 3a). The major rocks of the western NCA (Table 1) feed large talus slopes. Glacial plateaus, now deglaciated or nearly so, more than about a kilometer in extent are rare. A continuum of abandoned and vegetated to active talus aprons and cones (Fig. 4) is found from about 550 m to more than 2,500 m a.s.l. The eastern NCA, in contrast, are characterized by isolated massifs formed mainly of thick-bedded Dachstein Limestone (Table 1). These massifs are characterized by wider glacial plateaus, now deglaciated except for a few small remnants (Fig. 3b). Towards larger valleys, the plateaus descend in steep glacial chutes or by cliffs hundreds of meters in height. Talus slopes along the flanks of chutes and glacial plateaus tend to be comparatively small, low-dipping, and immature. Conversely, older, possibly late-Glacial alluvial fans and talus slopes situated down to more than 1,000 m in altitude below, along the toe of cliffs along larger valleys, are typically abandoned and vegetated. Because of dense jointing and ample intercrystalline pore space, the metadolostones of the CAM (Fig. 1; Table 1) weather under copious talus production. The subhorizontally bedded metadolostone successions form castellate summits separated by deep chutes and narrow

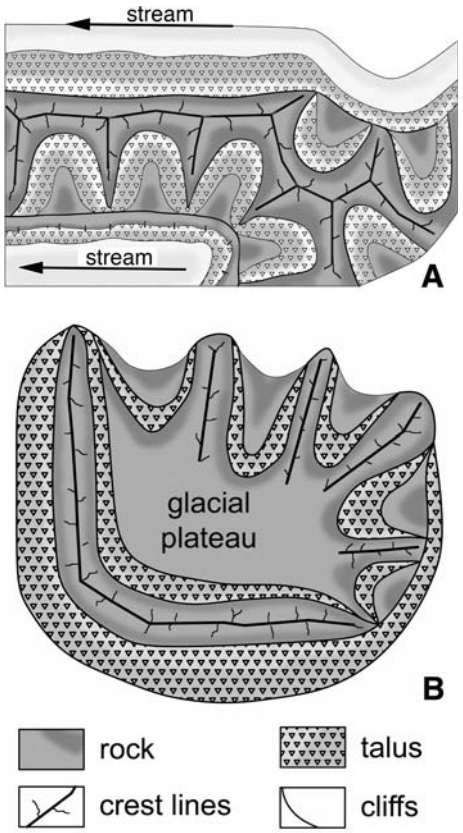

Fig. 3 Plan-view scheme of geomorphic characteristics of mountain massifs in the Northern Calcareous Alps. **a** The western Northern Calcareous Alps are characterized by W to E-trending mountain ranges. To the north, the ranges tend to have high cliffs or show glacial cirques. The southern side of the ranges typically consists of aligned glacial cirques to short hanging valleys. **b** In the eastern Northern Calcareous Alps, mountain massifs with more-or-less wide glacial plateaus are common. Along their northern and eastern side, the massifs debouch into valleys via glacial chutes. The western and southern sides are characterized by high cliffs

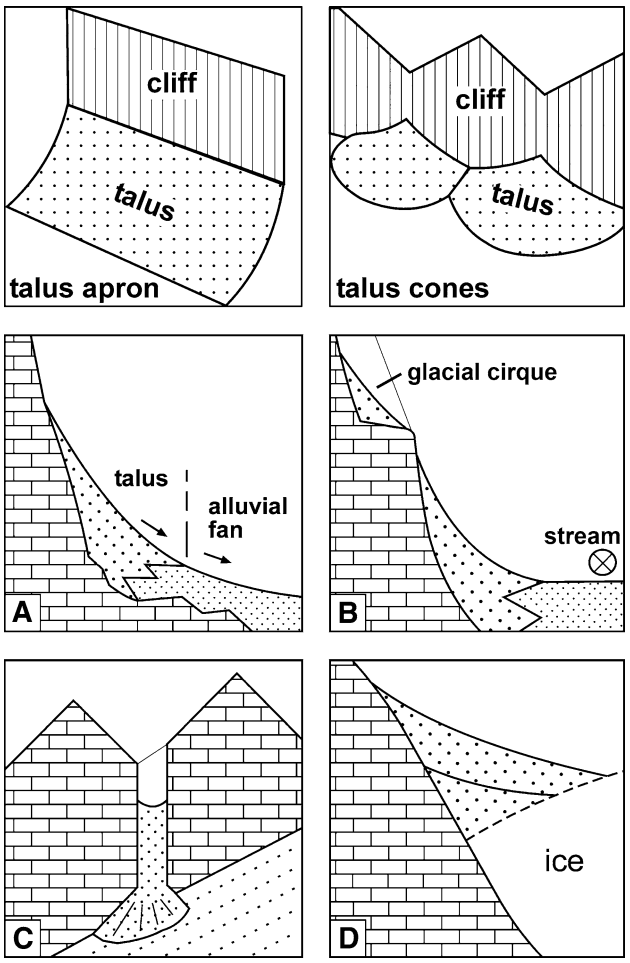

Fig. 4 Main forms and presence of talus slopes. Above Talus aprons (*left*) accumulate below rock cliffs of more-or-less planar shape. Talus cones (*right*) form below cliffs that are morphologically differentiated into chutes and gorges that focus clastic material to point sources. **a–d** Positions and depositional context of talus slopes. **a** Talus slope grades into alluvial fan farther down. **b** Talus slope along valley flank. In its distal portions, the talus interfingers with fluvial deposits. Higher up, glacial cirques provide local base-levels to talus slopes perched above the valley floor. **c** Chutes and gorges, typically between castellate summits, may be more-or-less filled by talus deposits. **d** In rare cases, lithified talus relicts of low depositional dip pinch out into air hundreds of meters above the present valley floor. These are interpreted as relicts of former ice-margin talus accumulations

Fig. 5 Active carbonate-lithic talus slopes, Eastern Alps (see Fig. 1 ▶ for locations). **a** Typical relation between fossil rock glacier (*r*, delimited by *dashed line*) and talus slopes. Up-slope of the rock glacier, in a morphological depression between rock glacier and talus slopes, a low-dipping rockfall-nourished 'basin-fill' (location labeled *x*) of cobbles to boulders accumulates. The talus slopes, in turn, are dominated by deposition from grain flows and rockfalls. *Scale bar* 200 m. Treffauer peak, NCA. *Source*: http://tiris.tirol.gv.at. **b** View up the east-facing talus slope of Lattenspitz (NCA). The cliff is comparatively low and of differentiated morphology. The talus slope is fed from a few point sources, and shows a steady increase in mean grain size from apex to toe. Width of view in foreground is about 40–45 m. **c** Fault-bounded block of Wetterstein Limestone (*WL*, Middle Triassic), shedding talus from its flanks. The north-facing cliff (*nc*) sheds onto a scree talus (*st*) which, in turn, debouches into the ephemerally active channel of a stream-dominated alluvial fan (*f*; only distal part of fan is visible in photo). The southern cliff (*sc*) is onlapped by a talus slope that, on its present surface, is dominated by gravelly grain flows (marked by *arrowtips*) and by rockfalls. Hüttenspitz, NCA. Compare with Fig. 7. **d** Relation between fluvial deposition and talus accumulation. The cliff is up to about 500 m in height. The talus apron ranges from 140 to 280 m in vertical height and is fed from numerous shallow chutes (point sources) in the cliff. Deposition and redeposition on the apron is mainly by debris flows. Along its toe, the talus apron downlaps onto and interfingers with fluvial deposits (*vf*). *Scale bar* 200 m. Stallen valley, NCA. *Source*: http://tiris.tirol.gv.at. **e** Talus cone dominated by cohesive debris flows. The talus cone is fed from a succession of metacarbonates that weather under copious production of mud-sized sediment. *Scale bar* 200 m. Hammerscharte, CAM. *Source*: http://tiris.tirol.gv.at. **f** West-facing cliffs of Kalkkögel group, CAM. The cliffs consist of Triassic metadolostones that weather out in chutes and narrow gorges, and under production of large talus cones (*t*) dominated by cohesive debris flows. Vegetated area (*r*) is a rock glacier. **g** 'Composite' talus slope. In the background, deposition dominated by alluvial processes gives rise to a talus fan (*tf*) with sieve-lobe complexes, sheet-flow deposits and channel incision (*arrowtip* labeled *c*). In the foreground, talus deposition is dominated by cohesive debris flows (*df*). The channel/levee ensemble labeled by *arrowtips* formed by a cohesive debris flow the night before the photo was taken on July 26, 2003. In addition, deposits of older debris flows prevail on this portion of the slope. Kalkkögel group, CAM. **h** Talus cone (*t*; delimited by *dashed line*) in onlap onto a rock cliff 700 m in height (not all in photo), and with a dip of 50–55°. The talus cone is 280 m in maximum vertical height, and dips with about 25°. Because the talus material is effectively removed by a perennial stream, this talus is kept in an immature stage of development. *Scale bar* 200 m. Pleisenspitz, NCA. *Source*: http://tiris.tirol.gv.at

gorges that focus downslope transport (cf. Gerber 1969; Cruden and Hu 1999). Except for talus slopes at or near the terminal stage, the CAM is characterized by debris-flow dominated talus cones.

Lithology and cliff shape

In terrains of compact thick-bedded limestones, talus slopes are comparatively poor in a matrix of carbonate-lithic sand to mud (Table 1), and are dominated by gravelly grain flows, gravelly hyperconcentrated flows, and rockfalls (Fig. 5a, b). Below cliffs that feed talus from their entire face and/or from closely spaced point sources, talus aprons developed (Fig. 5c, d). Most talus aprons are dominated by gravelly grain flows in their proximal part; farther down slope, cobbles to boulders derived from rockfalls (locally redeposited by snow avalanches, debris flows, or ephemeral fluid flows) prevail. Even below some of the highest and plane, north-facing cliffs of the NCA, however, no pure rockfall-dominated talus aprons developed; instead, chutes formed by surface runoff and by debris flows are intercalated. Only on rockfall-dominated

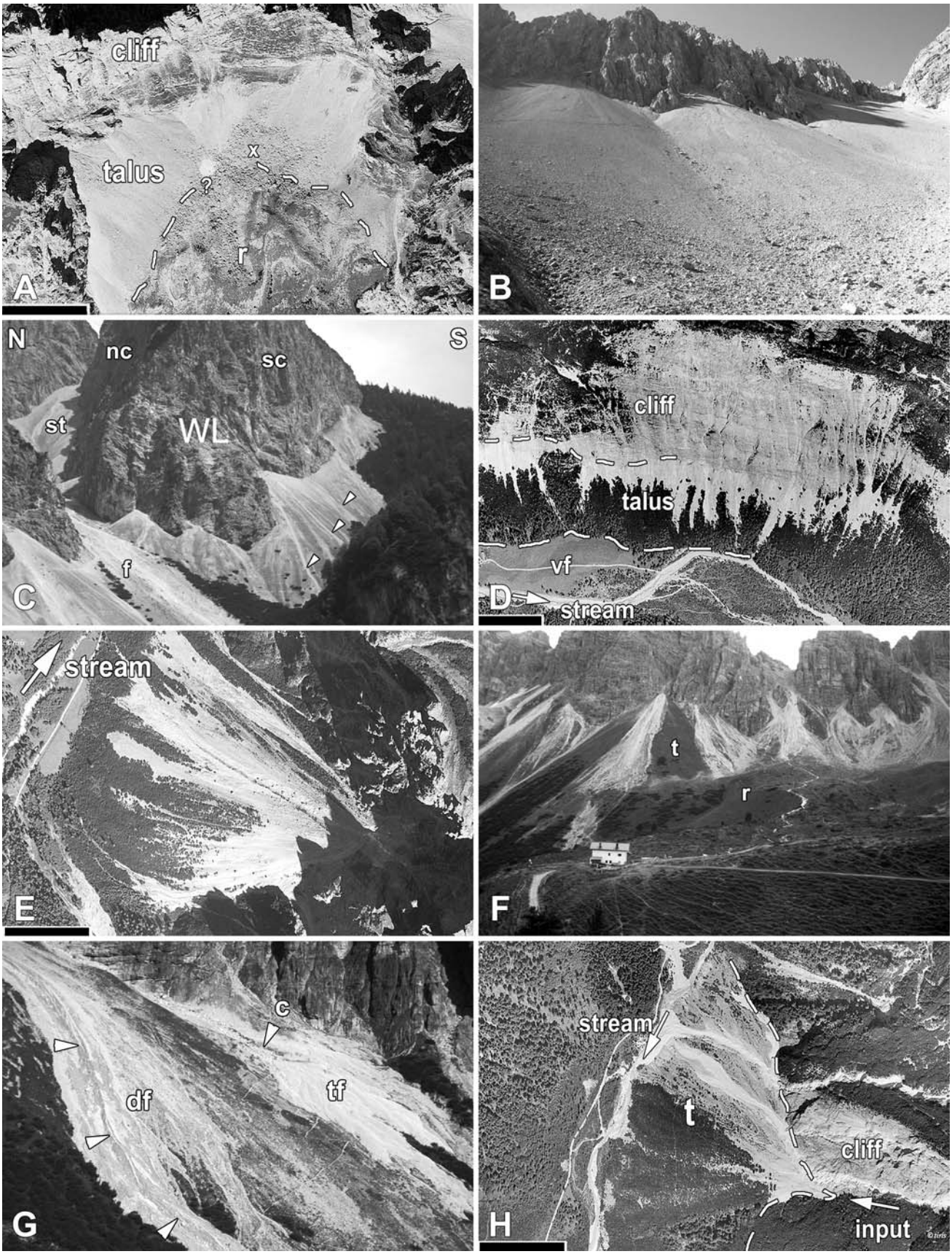
cliff
talus
x
?
r
A
B
N
nc
sc
S
st
WL
f
C
cliff
talus
vf
D
stream
stream
E
t
r
F
c
df
tf
G
stream
t
cliff
input
H

talus slopes characterized by *low* fall distance of clasts is rockfall the prevalent process of sediment delivery, transport, and final deposition.

Conversely, below cliffs differentiated by chutes or gorges that focus downslope transport to point sources, talus cones and/or alluvial fans developed (Fig. 5e, f). Talus cones dominated by cohesive debris flows are widespread in terrains of dolostones that typically are densely jointed and weather under copious production of gravel and sand- to mud-sized material. There is no sharp separation between alluvial fans and talus cones dominated by alluvial processes and/or by debris flows (compare e.g., Bones 1973; White 1981; Kotarba and Strömquist 1984; Whitehouse and McSaveney 1983; Ballantyne 2002, p. 161–162). Herein, we separate alluvial fans and talus cones by the amount and trend of slope dip from proximal to distal (see Appendix in supplementary material). High 'chuted' cliffs of compact limestone are typically onlapped by alluvial fans that may be viewed as an immature, early stage of talus slope development (cf. Fig. 2b, d). Conversely, cliffs of easily weathering dolostones are typically onlapped by large steep talus cones that may laterally merge into 'bajadas' (Fig. 5f). Active talus cones are dominated by ephemeral fluid flows and cohesive debris flows (Fig. 5g). On the cones, most downslope transport takes place by surface runoff during heavy rains, whereas snow avalanches and rockfalls are of minor importance. Deep gorges between castellate summits are typically filled by talus slopes that may dip with up to 50–60°. Where talus material is effectively removed by a stream ('basal removal'; Summerfield 1991), talus accumulation is either prevented, or the slope is kept in an immature stage (Fig. 5h).

Slope aspect

Abandoned and vegetated talus slopes are more common on south-facing mountain flanks. In structurally complex terrains such as the Eastern Alps, however, no straightforward relation between slope aspect and talus activity is to be expected (cf. Luckman 1976; Akerman 1984; Prick 1997). On north-facing mountain flanks, active talus slopes are widespread in altitudes above 1,400–1,800 m a.s.l. Along the toe of the north-facing talus slopes, protalus ramparts are common, and may be transitional into fossil rock glaciers (Fig. 6a). Fossil rock glaciers are widespread in cirques of the NCA (Figs. 5a, 6b), but well-developed protalus ramparts are limited to north-facing slopes. These ramparts may have formed in cooler climatic intervals during historical time. In the NCA, no entire talus slopes planed to 15–10° dip by passage of large avalanches of snow or slush was observed (avalanche roadbank talus; Gardner 1971; Luckman 1977; Whitehouse and McSaveney 1983). In contrast to high-latitude mountains characterized by rapid snowmelt and large slush avalanches (Theakstone 1982), in the present NCA, slush avalanches are too small to shape talus slopes. In the NCA, it is likely that most, if not all, rock glaciers are fossil. The age of the rock glaciers is poorly constrained. It is probable, however, that rock glaciers above 1,500–1,700 m a.s.l. are not mere late-glacial relicts, but formed newly or became re-activated during cooler climatic phases such as 'Little Ice-Age' type events.

Fig. 6 Active talus slopes and lithified talus successions, Northern Calcareous Alps. **a** Different development of NE- and SW-facing slopes. The talus below the NE-facing cliff developed as an apron fed by numerous point sources. Protalus ramparts (lobate, elongate bodies labeled by *arrowtips*) are situated directly upslope of a rock glacier (*r*). On the southwestern side, the rocky slope is of overall lower declivity, talus production is scarce, and protalus ramparts are absent. *Scale bar* 500 m. Rosskar peak, NCA. *Source*: http://tiris.tirol.gv.at. **b** Transition from glacial cirque (upper part of photo) into stream valley. Crestlines around the cirque are indicated by *barbed lines*. In the cirque, a fossil rock glacier (*r*) is downlapped by talus slopes (t_1) shed from the cliffs. The cirque is separated from the valley by a cliff. The cliff alongside the valley, in turn, is onlapped by talus aprons (t_2) in a lower position (cf. Fig. 4b). *Scale bar* 200 m. Samer valley, NCA. *Source*: http://tiris.tirol.gv.at. **c** Talus-alluvial fan ensemble. The talus slopes (*ts*) extend over a vertical distance of up to 400 m, and are separated by a slope knickline (*dashed line*) from active, lower-dipping alluvial fans (*af*) down slope. *Scale bar* 200 m. Zugspitzeck, NCA. *Source*: http://tiris.tirol.gv.at. **d** Detachment scar (*dashed heavy white line*) of a rockslide (*r, outlined by dashed thin white line*) that took place 4,000–4,500 years ago (Ostermann et al. 2007). Subsequently, the rock cliffs that flank the detachment scar became onlapped by talus slopes (*ts*) up to more than 500 m in vertical height. The talus slopes in the central and lower part of the photo merge, in physical continuity but separated by a slope knick line, into a lower-dipping alluvial fan (*af*). *Scale bar* 500 m. Fern Pass, NCA. *Source*: http://tiris.tirol.gv.at. **e** Detail of downslope-most portion of a lithified, rockfall-dominated fossil talus succession. The deposit is unbedded, shows isotropic clast fabric, is devoid of sedimentary structures, and consists of extremely poorly sorted sand to boulders up to a few meters in size. This deposit, about 100 m in thickness, consists entirely of lithoclasts shed from high cliffs from the present opposite (left) flank of the valley. *Hammer* is 35 cm in length. 1,240 m a.s.l., Eibental, NCA. **f** Lithified rockfall talus composed of angular to subangular fine gravels to boulders up to a few meters in size. The clasts are arranged in an isotropic clast fabric with a scarce matrix of carbonate-lithic sand. Width of view is 1.6 m. 1,370 m a.s.l., Hötting Breccia, NCA. **g** Detail of debris-flow dominated, partly cemented post-glacial talus succession (cementation age: 8.6 ka, Fig. 8b). Stratification (*dashed white lines*) dips with 15–20°. The succession consists of intervals of breccias with a matrix of unlithified lime mud, intercalated with calcite-cemented gravelly openwork strata. In addition, angular boulders (some marked by *arrowtips*) are intercalated. Width of view is about 25 m. 1,030 m a.s.l., Urschenbach, NCA. **h** Lithified scree talus dipping about 30° (stratification indicated by *dashed black line*). Note 'nest' of three small boulders, and the openwork lense (marked by *arrowtip*) of angular cobbles to coarse gravels directly upslope of the boulder 'nest'. *Hammer* is 35 cm in length. 1,490 m a.s.l., Hötting Breccia, NCA

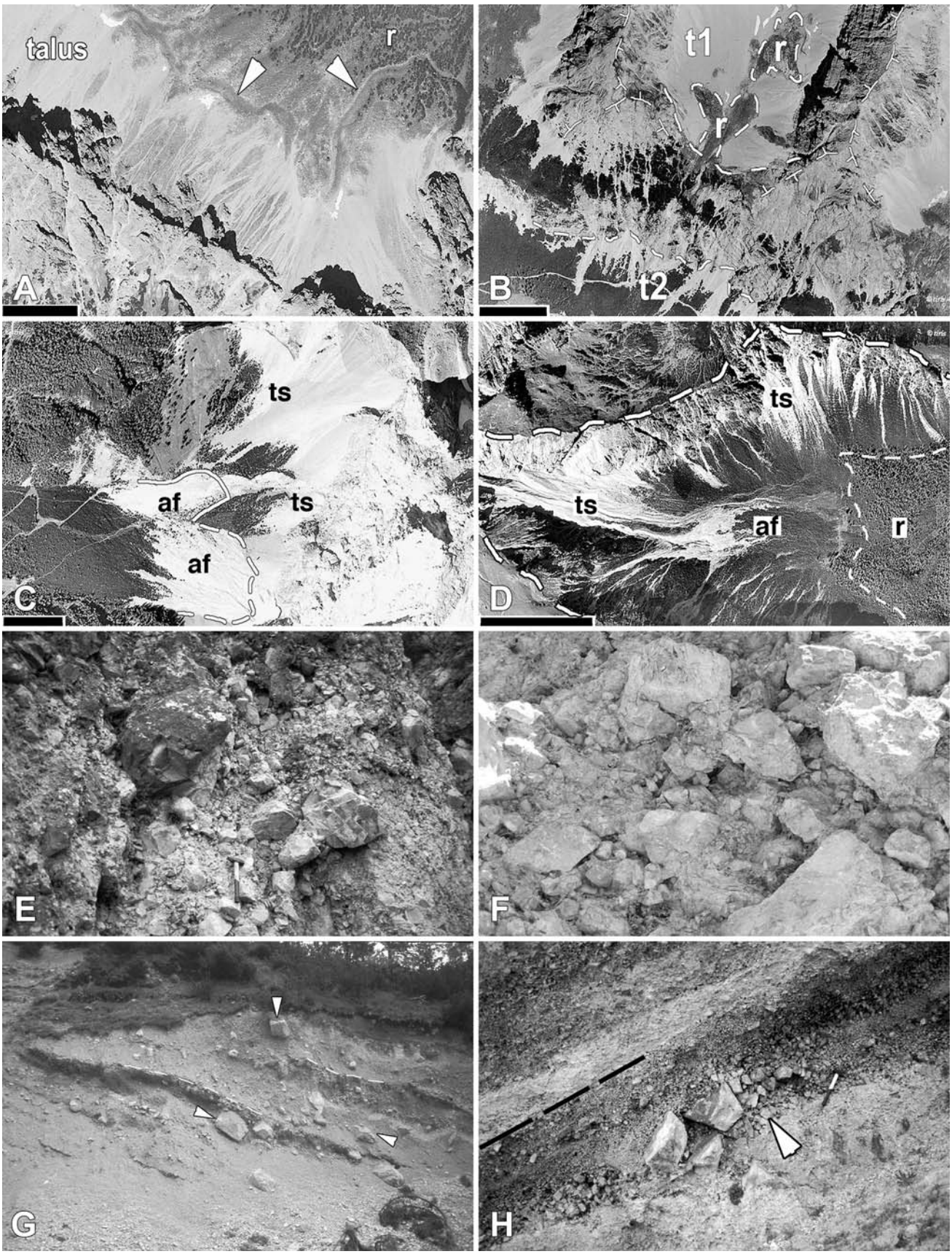
talus
r
A
t1
r
r
B
t2
ts
af
ts
af
C
ts
ts
af
r
D
E
F
G
H

Composite slope systems

Within a few square kilometers, local base-levels of talus slopes may differ by hundreds of meters in altitude (Figs. 4a–d, 6b). The proximal-distal gradient applies separately for each talus slope, and the same facies (e.g., grain flow breccias) can accumulate simultaneously in markedly different altitudes. In ancient talus relicts, therefore, facies types do not show a correlation with altitude above sea-level. Most taluses are present as a single slope from apex to toe. In contrast, 'composite systems' consist of different deposystems in a row one after the other (Figs. 5c, 7), and/or of several talus slopes fed from different cliffs but merging into a single larger slope (Fig. 5g). In the NCA, active talus slopes shedding onto active alluvial fans (Fig. 4a) seem relatively uncommon, but this is largely due to inactivity or low activity of many of these systems nowadays. Below high cliffs, active talus-alluvial fan ensembles persist until the present (Fig. 6c). Along valley flanks denuded by post-Glacial rockslides (e.g., Tschirgant, Patzelt and Poscher 1993; Fern Pass, Ostermann et al. 2007), talus slope-alluvial fan ensembles rapidly accumulated after rocksliding (Fig. 6d). In these systems, the steeper-dipping surface of talus is separated by a knick in slope from the surface of the alluvial fan.

Valley-flank successions

In the NCA, in altitudes normally between 500 and 1,000 m a.s.l., gravel pits and natural outcrops expose late-glacial to post-glacial successions (Fig. 8). In some outcrops, a basal interval of glacial lodgement till or redeposited till is present above a truncated rock substrate. Above, cohesive debris-flow deposits with or without glacially derived clasts may be present, and are overlain by a talus succession.

Lithified talus successions: facies

Rockfall deposits

Two types of rockfall deposits are distinguished (Table 2):

1. Extremely poorly to poorly sorted clast-supported openwork breccias composed of boulders to coarse carbonate-lithic sand (Fig. 6e, f). The boulders to gravels are of angular to subangular shape; the sand grains range in rounding from angular to subrounded. In the outcrop, no bedding or vertical and lateral segregation of clast size is obvious. The [a, b]-axial planes of cobble- to boulder-sized, elongate or platy, clasts locally may show an indistinct preferred orientation subparallel to the former depositional surface. In these breccias, matrix is scarce, and is a carbonate-lithic sand to silt that only locally fills smaller interstices. Below larger platy clasts, open megapores are present. Locally, a secondary infiltrated matrix of geopetally laminated carbonate-lithic sand to lime mudstone is present.
2. Within other talus facies, isolated angular cobbles to boulders may be intercalated in 'clast trains' (Fig. 6g). Along a clast train, clast size typically is highly variable. Such clast trains were observed in the low-dipping distal part of fossil talus slopes. In addition, isolated boulders or 'nests' of a few boulders were observed within finer-grained talus breccias, in the proximal sector of fossil talus slopes. Directly upslope of these boulders, lenses of openwork breccias composed typically of cobbles to coarse gravels are present (Fig. 6h).

Interpretation

Herein, we designate rockfall-produced talus facies as those deposits that were fed by *and* accumulated from rockfalls. Immature rockfall-dominated talus slopes are characterized by relatively gentle dip (up to about 20°), and by poor segregation of clast sizes, giving rise to isotropic clast fabric (Clowes and Comfort 1987; Pérez 1989). On mature rockfall-dominated talus below high cliffs with a large mean fall distance of clasts, the higher inertia of larger clasts enables farther downslope transport (Statham 1976); in addition, a 'sieve effect' (Brückl et al. 1974) and selective entrapment of smaller clasts upon talus shift (Gardner 1979) support upslope-downslope segregation of clast sizes. Mature rockfall-nourished talus slopes thus commonly show smallest mean grain size and best sorting in their proximal part, and an overall gradual transition to less sorting and larger mean grain size towards their distal part. Although the proximal part of such slopes may be fed mainly by rockfalls, the prevalent mode of subsequent downslope transport and final deposition is by grain flows and particle creep, such that the resulting deposits do not represent a rockfall facies as understood herein.

The type 1 breccias accumulated in the distal/basal part of talus slope successions. This interpretation is suggested by the extremely poor sorting of the breccias, combined with their isotropic openwork fabric, absence of bedding, and their low topographic position either relative to associated talus facies and/or relative to local base-level (Fig. 9a, b). Type 2 rockfall deposits, i.e., the clast trains, probably result from a single or a few rockfall events. Such

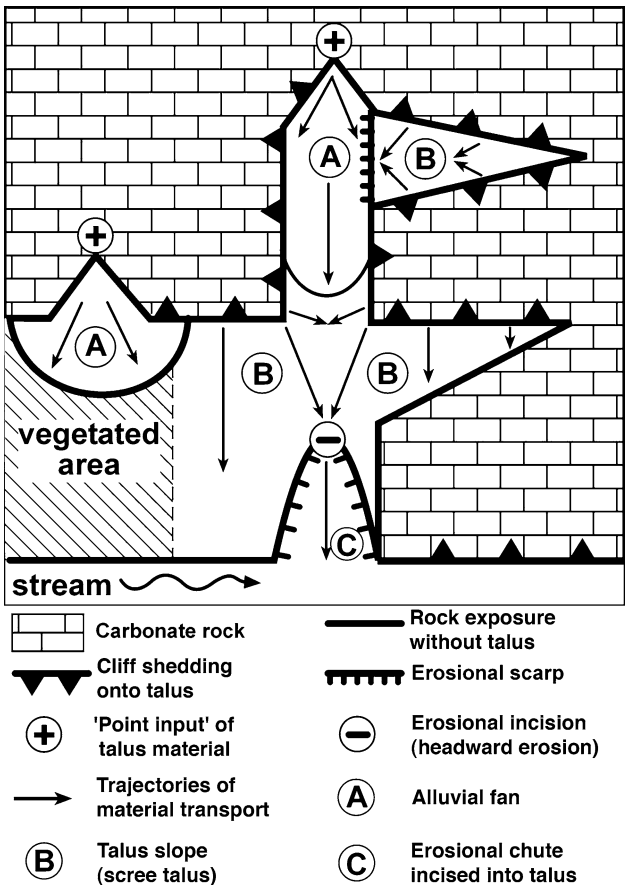

Fig. 7 'Composite slope system' of different coarse-clastic deposystems. A stream-dominated alluvial fan (**a**) is point-fed by clastic material shed from a chute in a high cliff. Downslope, because of percolation of water into the talus accumulation, the fan depositional system grades into a distinctly steeper-dipping scree talus (**b**). The scree talus is dominated by grain flows. Still farther down slope, because of groundwater re-emergence from the talus, a steep erosional chute (**c**) became incised by headward erosion. Compare with Fig. 5c

layers are obvious only if they are intercalated into talus facies of different characteristics. Alternatively, at least some of the clast trains originated from transport in snow avalanches (cf. Gardner 1970; White 1981; Francou and Manté 1990; Jomelli and Bertran 2001). In fossil talus successions, to date we could not identify a clast train unambiguously formed by snow avalanche transport. In the upper part of fossil talus slopes, the isolated outsized boulders intercalated in successions of finer-grained grain flow breccias either were transported to the site by snow avalanches, or represent rockfalls stopped by a snow cover.

Grain flow breccias

Openwork breccias deposited from gravelly grain flows comprise a significant portion of the proximal part of lithified talus successions (Fig. 9c, d; Table 2). The breccias are present in subparallel beds 20–50 cm in thickness that typically dip 30–35°. In dip section, individual beds are slightly wavy to undulose, and laterally persist over a few meters to a few tens of meters. In strike section, beds are lenticular. Up-slope within this facies, a steepening of bedding is observed from about 20–25° (Fig. 9e) to predominantly 30–35° (Fig. 9c). Bedding dip between 30–35° may extend over hundreds of meters up slope. In packages dominated by this facies, stratification is obvious (Fig. 9d, f), but bedding surfaces tend to be unsharp. Bedding is visible because of: (a) slight vertical changes in mean grain size and sorting; (b) intercalated beds of breccias deposited from cohesive debris flows with a primary matrix of lime mud (Fig. 9f, g); or (c) intercalated beds with a secondary matrix of geopetally infiltrated carbonate silt to mud (Fig. 9h). Locally, unstratified intervals up to a few meters thick are present (Fig. 10a). Beds typically consist of very poorly to well-sorted, angular to subangular, fine gravels to cobbles in openwork fabric (Fig. 10b). The [a,b]-axial plane of platy clasts commonly is subparallel to stratification. In addition, both downslope and upslope clast imbrication was observed (Fig. 10b). Up-slope from the lower, low-dipping (20–25°) occurrence of this facies, a trend towards better sorting and a decrease in mean grain size is obvious.

Interpretation

The described sediment characteristics all suggest that these breccias accumulated from grain flows (cf. Allen 1970, p. 327; Statham 1976; Church et al. 1979; Pérez 1989). On recent talus slopes, grain flows form discrete tongues a few meters to hundreds of meters in downslope extent; these grain flow tongues show an elevated margin (Fig. 10c). The upslope portion of individual grain flows is the most fine-grained, consisting usually of coarse sand to fine gravel. Down slope, over the largest part of grain flow tongues, the sediment is typically a medium to coarse gravel with a few clasts up to cobble size (Fig. 10d). At the snout of grain flows, a comparatively coarser-grained openwork of coarse gravel to small boulders may be present, or the flow halted upon run-up onto cobbles to boulders (Fig. 10e).

In the described breccias, the 'trains' of down-dip imbricated clasts originated by upflow propagating shear during freezing of the grain flows. On recent talus slopes, grain flows may proceed in either dry or wet clastic material, and can be triggered by various processes such as passing deer or man, rockfall impact, intense rain, or water chuting down cliffs during rainstorms. Although some of the breccia beds might have originated from frost-coated clast flows (e. g. Fig. 9e) (FCCF, Hétu and Gray 2000), we did not find unequivocal positive evidence for a prevalence

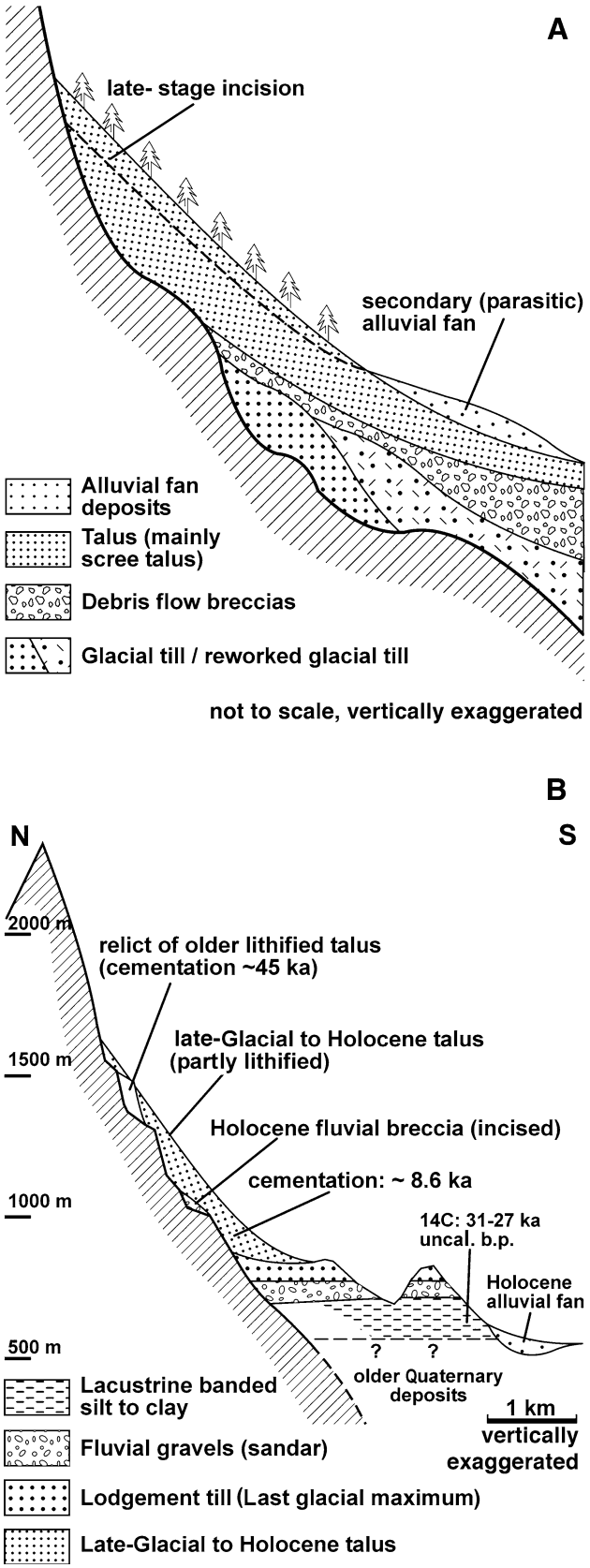

Fig. 9 Facies of carbonate-lithic talus slopes, Eastern Alps. **a** Man-made excavation into rockfall-dominated talus. The talus consists of extremely poorly sorted, angular fine gravels to small boulders arranged in an isotropic clast fabric. The clasts are thinly coated by a 'dusty' matrix of carbonate-lithic sand to micrite. Pen is 14 cm in length. Gravel pit 'Goidinger I', NCA. **b** Upslope view onto distal, low-dipping part of rockfall-dominated talus. Note composition mainly of angular cobbles to boulders, lack of clast size segregation, and isotropic clast fabric. Excavation revealed openwork clast fabric down to at least about 80–100 cm below the surface. 2,010 m a.s.l., below Mandlspitz, NCA. Width of view is about 15 m. **c** Lithified scree talus composed of openwork breccias deposited from grain flows. Stratification (indicated by *dashed white line*) is visible because of strata composed of angular-subangular gravels of different mean diameter. Pen is 14 cm in length. 1,570 m a.s.l., Hötting Breccia, NCA. **d** Lithified scree talus, with strata dipping about 30°. This succession consists of, both, strata of openwork breccias deposited from gravelly grain flows and of matrix-bearing clast-supported breccias deposited from cohesive debris flows. Width of view is about 10 m. 1,450 m a.s.l., Hötting Breccia, NCA. **e** Detail of distal part of debris-flow dominated, partly lithified post-glacial talus succession (detail of Fig. 6g). Stratification dips with about 20°. A bed of breccia with a primary matrix of unlithified lithic lime ooze is overlain by a bed of partly cemented openwork breccia. *Pen* is 14 cm in length. 1,030 m a.s.l., Urschenbach, NCA. **f** Lithified scree talus composed of backweathering strata of openwork breccias deposited from grain flows (*gf*), of intercalated outweathering levels a few centimeters in thickness of geopetally infiltrated secondary matrix (labeled by *arrowtips*), and of a resistant bed (*cdf, base indicated by dashed white line*) of clast-supported breccia with a primary matrix of lime mudstone, i.e., a bed that was deposited from a cohesive debris flow. Width of view is 1.70 m. Tawald, NCA. **g** Detail of lithified scree talus. A layer of extremely poorly sorted, gravelly to small-bouldery openwork breccia deposited from grain flow (*gf*) is under- and overlain by intervals of extremely poorly sorted cohesive debris-flow breccias (*cdf*) with a primary matrix of lime mud. Width of view is 1.6 m. 1,465 m a.s.l., Hötting Breccia, NCA. **h** Detail of lithified scree talus. Stratum of openwork breccia (*ob*) deposited by gravelly grain flow, topped by an interval wherein the interstitial pore space became filled by infiltrated, geopetally laminated secondary matrix (*gsm*). Top of stratum with secondary matrix labeled by *dashed white line*. *Pen* is 14 cm in length. Tawald, NCA

Fig. 8 Successions closely above the present floor of larger valleys, Northern Calcareous Alps. **a** Above a rock surface shaped by subglacial erosion, erosional relicts of (redeposited) glacial till may be overlain by debris-flow breccias. The breccias, in turn, are overlain by a talus slope. In many cases, the talus slope is incised by a channel that, downslope, either grades into an alluvial fan (as shown), or that debouches into a stream. **b** Section through succession along left flank of valley east of Innsbruck (location 25 in Fig. 1; Ostermann 2006). Lacustrine deposits (^{14}C ages of organic remnants 31–27 ka uncal. b.p.; Fliri et al. 1970) are overlain by proglacial fluvial gravels and, above, by lodgement till of the Last Glacial Maximum. The till, in turn, is downlapped by an alluvial fan-to-talus succession. A U/Th cementation age of 8.6 ka suggests that the fan/talus ensemble accumulated soon after deglaciation of the valley at about 17 ka. Today, the fan/talus ensemble is subject to linear erosion

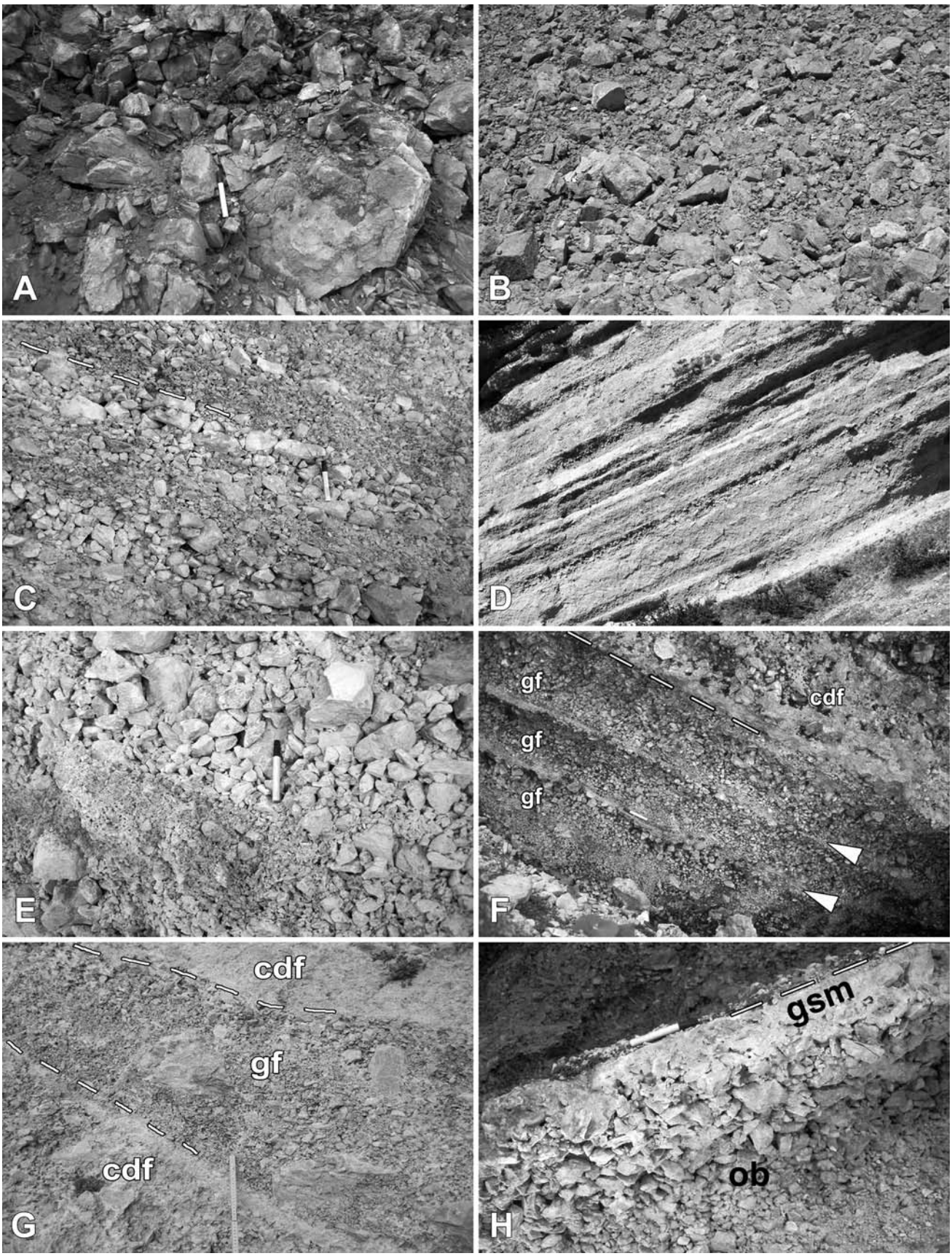
A
B
C
D
E
gf
cdf
gf
gf
F
cdf
gf
cdf
G
gsm
ob
H

Table 2 Prevalent facies of carbonate-lithic talus slopes, Eastern Alps

Facies	Description	Dip of beds	Position	Interpretation	Remarks
Rockfall breccias	(1) Very indistinctly bedded to typically unbedded, extremely poorly to very poorly sorted, clasts angular, isotropic clast fabric, no primary matrix (2) Upper part of talus: isolated layers only	(1) Lower part of talus: 10°–25°, bedding hardly recognizable (2) Upper part of talus: 30°–35°, up to 45°	(1) Intervals up to about 100 m thick: basal and lower part of talus (2) Isolated layers: upper to lower part of talus	Breccias deposited from rockfalls	(1) Rarely preserved and exposed (2) Commonly associated with or mixed into other facies
Grain flow breccias	Subparallel dm-to xdm-bedded, poorly to well-sorted fine gravel to cobbles, clasts angular-subangular, no primary matrix. May contain geopetally laminated secondary matrix of lime mudstone	Commonly 25°–35°, up to 40° Less commonly down to 20° (frost-coated clast flows?)	Successions in upper part of talus	Breccias deposited by grain flows (cohesionless debris flows), overprinted by particle creep	Widespread to prevalent
Breccias to conglobreccias of matrix-bearing (cohesive) debris flows	Very poorly to extremely poorly sorted, bedding planes indistinct and a few centimeters to a few meters vertically apart, intervals lenticular, gravels to boulders angular to subrounded, clast- to matrix-supported, matrix of lime mud to silty-sandy lime mud	A few degrees to 30°	Upper to lower part of talus	Breccias to conglobreccias deposited by cohesive debris flows with a fine-grained matrix	Widespread to prevalent In detail highly variable
Breccias to conglobreccias deposited from fluid flows	(1) Channel-fills: Unbedded, lenticular intervals of extremely poorly to poorly sorted, angular to rounded fine gravels to boulders, clast openwork or matrix of winnowed sand, clasts parallel to bedding and imbricated cobbles to boulders, locally downward-convex bedding planes and beds. Underclast pores widespread	Few degrees to about 20°	Lower to middle part of talus	Deposited in channels during ephemeral (torrential) surface runoff	Relatively common Confined to a single bed or a few stacked beds intercalated into successions dominated by other facies
	(2) Sheet-flow deposits (sieve lobes) Packages of distinctly subparallel stratified, moderately to well-sorted openwork gravel to sand, arranged in stacked gravel/sand rhythms	Few degrees to about 20°, rarely up to 30°	Commonly in distal (lower) part of talus slopes Talus cones with abundant surface runoff may contain this facies also in the proximal (upper) part of slope	Sieve lobes deposited from sheet flows during waning stage	Common to prevalent Stacked sieve lobes build terraces alongside channels
Bouldery rock glacier breccia	Unbedded, extremely poorly sorted, clast-supported deposit of lithic sand to boulders, isotropic clast fabric, clasts angular to subrounded, matrix is (chalky) non-laminated ocre-colored lime mudstone, matrix content somewhat variable in patches within deposit	Not recognizable	Basal part of talus	Deposit represents the vestige of a rock glacier that formed and, later, melted during deglaciation	To date interpreted in a single succession

of FCCF deposition. An additional process of downslope transport on slopes of cohesionless clasts is particle creep or 'talus shift' (Selby 1985). Talus shift is triggered by several processes such as rain and snowmelt, snow drag, rockfall impact, passing deer and man, and diurnal hot/cold-changes (Rapp 1960; Gardner 1979; White 1981). Whereas the rate of downslope creep of individual clasts is variable (0–71 m/year; Gardner 1979), over decades, talus shift leads to wholesale downslope creep with a few centimeters to more than a meter per year (Gardner 1979). No sedimentary structures or clast fabrics diagnostic of talus shift are known. The effect of particle creep may be to overprint sedimentary structures produced by grain flows.

Rudites of cohesive debris flows

These include breccias to conglobreccias that are most commonly clast-supported and contain a matrix of lime mudstone to carbonate-lithic wackestone to packstone (Fig. 10f, g). The matrix content ranges from pore-filling to only partly pore-filling. Vertically across beds, no segregation of clast size is obvious, and sorting typically is poor to extremely poor. Inverse grading in the basal part of beds, and projecting boulders at bed tops may be present (Fig. 10h). In breccias with pore space only partly filled by matrix, polished slabs and thin sections suggest that partial pore-fill, at least in part, results from eluviation after deposition (Figs. 10g, 11a). In many cases, the matrix is riddled by secondary macropores; these macropores are, in turn, completely or partly filled by a laminated, geopetally infilled secondary matrix of calcimicrite to -siltite similar to the primary matrix. In a few bedsets at various locations, the matrix of these breccias is rich in micas and metamorphic rock fragments derived from glacial drift.

In this facies group, two types are distinguished:

1. Poorly to extremely poorly sorted, clast-supported, gravelly to bouldery breccias that typically comprise beds up to a few meters thick (Fig. 11b). In packages of such breccias, bedding planes commonly are indistinct and laterally grade into amalgamation surfaces with vertically adjacent beds. In breccias of this facies type, bedding dips range from subhorizontal up to about 25°. In low-dipping successions (up to about 10°), the base of breccia beds typically is non-erosive to gently erosive. In successions with a steeper dip (10–25°), in strike section, bedding typically is lenticular on a lateral scale of meters to a few tens of meters.
2. Clast-supported breccias of well- to moderately sorted, angular to subangular fine to coarse gravel, and with the pore space filled by matrix. These breccias are present in beds that, in the dip section, are undulating and lenticular, and are a few decimeters to, rarely, more than 1 m thick. In the strike section, some of the beds are distinctly lenticular. Beds of these breccias dip with a few degrees up to 35°. In none of the investigated talus slope successions, entire beds of matrix-supported breccias have been observed, i.e., beds that would pertain to the mud-flow class of debris flow rheology. If present, matrix support is confined to small lenses and pockets within a few breccia beds. In Pleistocene lithified hillslope successions of the Eastern Alps, pebbly mudflows are rare and, as far as documented, accumulated in depositional systems different from talus slopes (Sanders and Ostermann 2006).

Interpretation

The described characteristics of breccias of facies (1) indicate that these breccias were deposited from debris flows with matrix shear strength ('cohesive debris flows') (cf. van Steijn 1988; Nieuwenhuijzen and van Steijn 1990; Bertran et al. 1995; Allen 1997). On recent Alpine talus slopes, gravelly debris flow deposits with a matrix content of only a few percent are common (e.g., Van Steijn 1988, and own obs.). For extremely poorly sorted sediment, up to more than 95% in volume can be clastic material before grain interlocking occurs (Rodine and Johnson 1976). Thus, at least many of the flows giving rise to clast-supported breccias with a primary matrix may have moved as Bingham fluid, or largely so, combined with a dilatant flow component (Hampton 1979).

The breccias of facies (2) are interpreted as deposits of cohesive debris flows with a better-sorted gravelly clast fraction than the preceding facies. In the talus successions, the absence of beds of matrix-supported debris flow breccias is not related to paucity of carbonate mud. Mud-sized sediment indeed is a significant constituent of carbonate-lithic talus slopes. On the talus slopes, however, no processes that would result in significant accumulation of mud at the surface of the slope, to sustain potential mud flows, are active.

Fluid flow deposits

On recent talus slopes and in their lithified counterparts, fluid flow deposits include diverse ruditic to lutitic sediments that typically prevail in the distal part of slope. Deposition from fluid flows may range from rare events of surface runoff that significantly overprint the slope to the development of stream-dominated talus cones. Talus cones may nourish stream-dominated alluvial fans directly down slope. In the following, the two most widespread facies of fluid flow deposits on talus slopes are described.

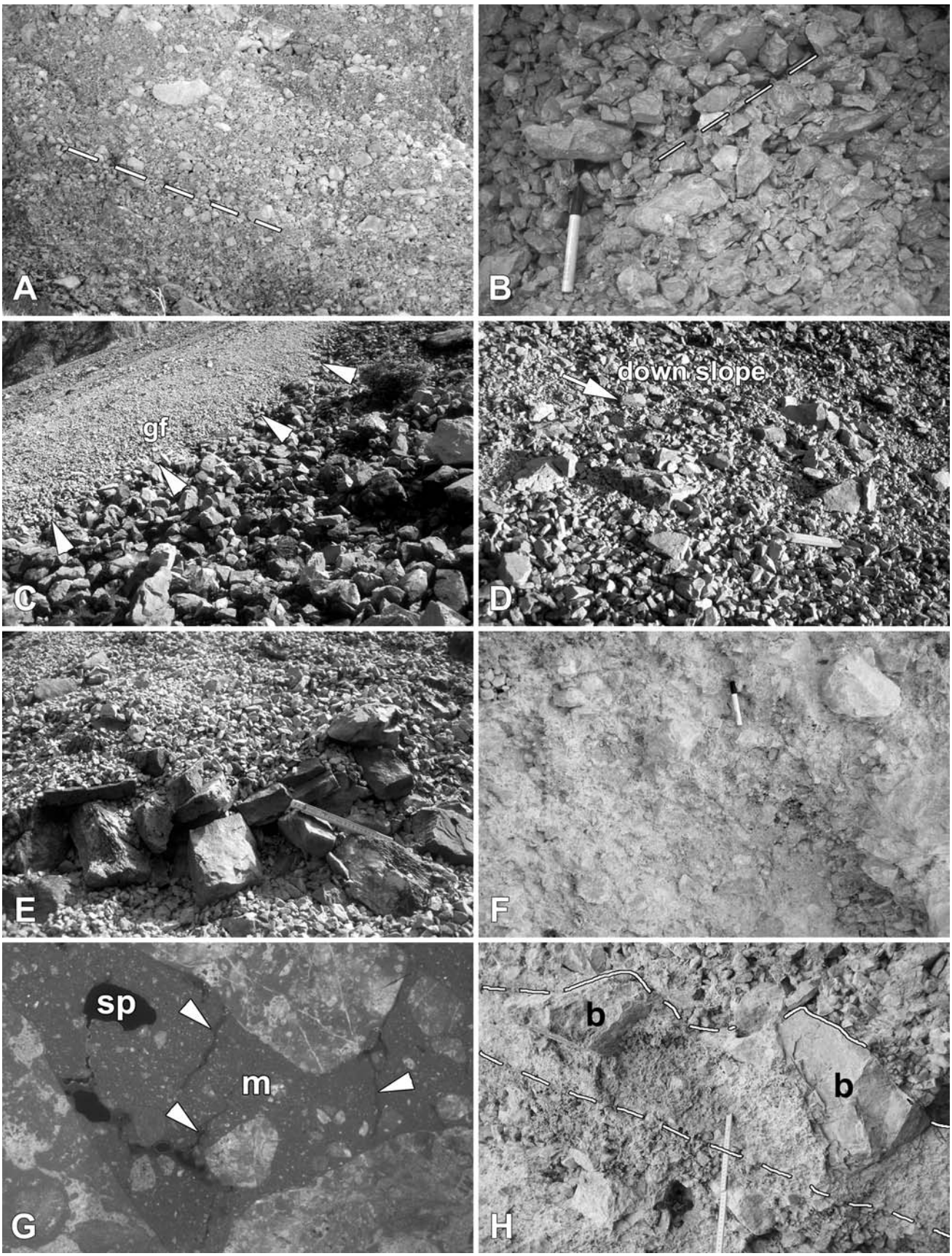
A
B
gf
C
down slope
D
E
F
sp
m
G
b
b
H

◄ **Fig. 10** Facies of carbonate-lithic talus slopes, Eastern Alps. **a** Lithified scree talus. Detail of an interval about 8 m in thickness composed of unstratified to faintly stratified, moderately sorted, gravelly openwork breccias with a few intercalated cobbles (apparent dip of stratification indicated by *dashed line*). The gravels to cobbles are preferentially arranged with their (a,b)-axial planes subparallel to the former talus slope surface. Width of view is 4 m. 1,550 m a.s.l., Hötting Breccia, NCA. **b** Lithified scree talus of openwork breccias deposited from grain flows. Overall dip of stratification indicated by *dashed white line*. Note very poor sorting, orientation of (a,b)-axial planes of clasts subparallel to stratification (= former surface of talus slope), and presence of downslope-imbricated clast fabrics (*above pen*). *Pen* is 14 cm in length. Tawald, NCA. **c** Lateral margin (labeled by *white arrowtips*) of grain flow deposit (*gf*). The grain flow had been shed over an older, coarser-grained talus surface composed of cobbles to small boulders. Width of view in foreground is about 4 m. Talus below Hüttenspitz, Karwendel. **d** Surface of grain flow deposit shown in the preceding figure. The surface is relatively plane, but is riddled by cobbles that stayed afloat on the moving mass of gravelly sediment. Width of view in foreground is 1 m. **e** Detail of distal part of gravelly grain flow deposit (labeled by middle *arrowtip* in Fig. 5c). The central portion of the grain flow had been 'ponded' against an array of older, angular cobbles. *Scale bar* is 22 cm in length. Compare with Fig. 6h. **f** Breccia deposited from a cohesive debris flow: clast-supported, extremely poorly sorted breccia with a primary matrix of lime mudstone. *Pen* is 14 cm in length. 1,490 m a.s.l., Hötting Breccia, NCA. **g** Thin-section photomicrograph of a clast-supported conglobreccia deposited from a cohesive debris flow. The deposit consists of clasts of shallow-water limestones within a primary matrix (*m*) of carbonate-lithic wackestone. In the matrix, note open solution pores (*black patches, sp*) and small cracks (labeled by *arrowtips*) that are oriented subnormal to clast surfaces. Width of view is 17 mm. Crossed nicols. 1,350 m a.s.l., Ahornboden-Hohljoch breccia, NCA. **h** Detail of scree talus. Bed of cohesive debris-flow breccia (indicated by *dashed white line*) of very poorly sorted carbonate-lithic sand to coarse gravels, and with a few small boulders (*b*) that project from the top of the bed. The bed is sharply intercalated between strata of openwork breccias that accumulated from grain flows. Width of view is 1.4 m. 1,470 m a.s.l., Hötting Breccia, NCA

1. Channel-fills: Breccias to conglobreccias deposited in channels with ephemeral runoff comprise intervals a few decimeters to a few meters thick (Fig. 11c–f). In the strike section, the base of the intervals is incised into underlying deposits in a climbing and falling pattern, and the intervals show a lenticular cross section (Fig. 11f, g). In the dip section, most clasts of gravel to cobble size are oriented with their [a,b]-axial plane subparallel to bedding, but short 'trains' of typically two to four downstream-imbricated cobbles to boulders are locally present (Fig. 11h). The deposits consist of extremely poorly sorted rudites of gravels to boulders. Within an interval, rounding of boulders typically is variable from angular to well-rounded. The rounding of the cobble- to gravel-size fraction typically ranges from subangular to subrounded. The matrix is a winnowed, medium- to coarse-grained carbonate-lithic sand (Fig. 12a). In framework pores between clasts, the matrix shows a characteristic geopetal arrangement of grain size. Above the primary matrix of winnowed medium to coarse sand, upward-fining layers a few millimeters to a few centimeters thick of fine-grained carbonate-lithic sand to mud are present (Fig. 11h). The upward-fining layers may show parallel geopetal lamination, or upward fining is continuous (Fig. 12a).
2. Sieve lobes: Breccias to conglobreccias accumulated from unchannelized flow (sheet flow) are vertically associated with channel deposits as described above (Fig. 11c). They consist of poorly to well-sorted coarse- to medium-grained openwork gravel to coarse sand with distinct subparallel bedding (Fig. 12b). Clast rounding commonly ranges from subangular to subrounded, and the matrix is a winnowed carbonate-lithic sand (Fig. 12c). Bedding is mainly defined by vertical changes in mean grain size. Individual beds are a few centimeters to about 50 cm in thickness, and are characterized by upward-fining from medium gravel (less commonly coarse gravel) at the base to fine gravel or coarse sand at the top. In the gravelly layers, downstream imbrication is common, but most gravels are oriented with their [a,b]-plane subparallel to bedding. In the upper, sandy part of the beds, the sand may show subparallel lamination, and a few 'outsize' clasts of gravel to cobble size may be intercalated in the upper sandy part of beds. Beds of this facies commonly occur in rhythmically stacked packages a few decimeters to a few meters thick. Bedding dip ranges from subhorizontal to about 15°, rarely up to about 20°.

Interpretation

The presence of fluid flow deposits in the distal sector of talus slopes results from surface runoff and groundwater emergence mainly during snowmelt and during heavy rains. Carbonate-rocky talus prone to surface runoff is characterized by richness in fine-grained matrix. Such talus is common on dolostone terrains, where rainstorms readily trigger cohesive debris flows and redeposition of talus material in ephemeral creeks and by slope wash. Alternatively, fluid flow deposition may result from focusing of surface runoff down from the rock cliff.

In outcrop, extremely poorly sorted deposits of torrents may look similar to those of cohesive debris flows. This is because (a) channel re-activation during build-up of floods may be separated by weeks to years, and (b) rapid deposition during waning flood commonly leaves too little time for the ephemeral torrential channels to acquire all the characteristics of perennial proximal fluvial channels (cf. Montgomery and Buffington 1997). Distinction of torrential channel-fills from debris flows is

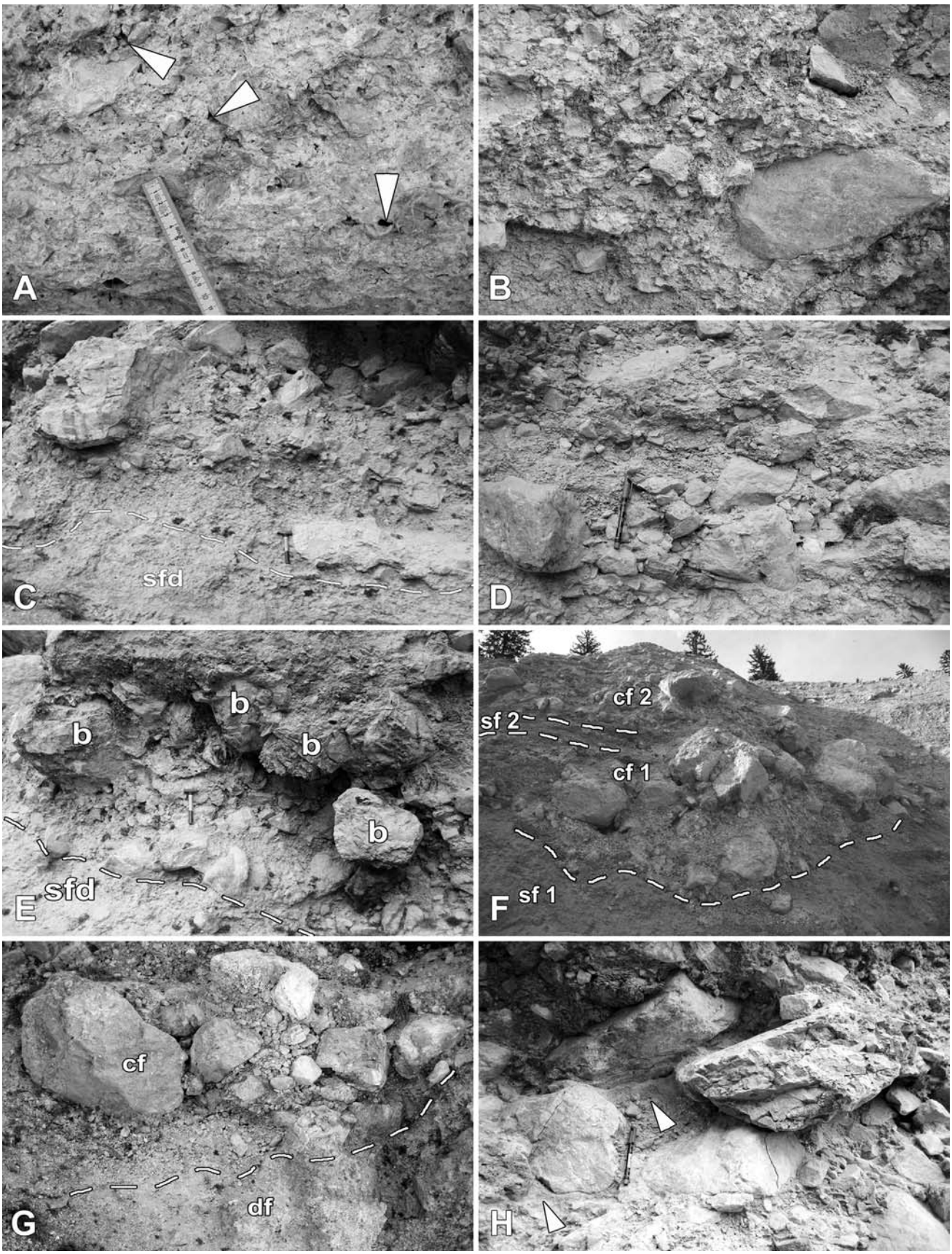
A
B
C
sfd
D
b
b
b
b
sfd
E
cf 2
sf 2
cf 1
sf 1
F
cf
df
G
H

◀ **Fig. 11** Facies of carbonate-lithic talus slopes, Eastern Alps. **a** Detail of bed of clast-supported breccia composed of fine gravels to cobbles embedded in a primary matrix of lime mudstone. The matrix is riddled by macropores (a few labeled by *arrowtips*) up to more than a centimeter in width. *Scale bar* in cm. 1,470 m a.s.l., Hötting Breccia, NCA. **b** Detail of breccia bed composed of angular to subrounded gravels to small boulders, embedded in a matrix of carbonate-lithic wackestone to siltstone. Width of view is 2 m. 1,180 m, Hötting Breccia, NCA. **c** Detail of succession dipping with 8–15°, and that provides the foundation to 30–35° dipping scree talus slopes higher up-section (see Fig. 13). In the lower part of the outcrop, gravelly/sandy rhythms deposited from sheet flows (*sfd*) are present. The sheet-flow deposits, in turn, are overlain along a surface of erosion (indicated by *dashed white line*) by an interval of bouldery breccia to conglobreccia that accumulated within an ephemerally active torrent channel. *Hammer* is 35 cm in length. 1,350 m a.s.l, Hötting Breccia, NCA. **d** Detail of channel fill shown in **c**. Note presence of both rounded and subangular clasts. *Pen* is 14 cm in length. **e** Detail of dip section of filling of ephemerally active torrent channel. The base of the interval (marked by *dashed line*) is incised into finer-grained and better-sorted gravels and sands deposited from sheet flows (*sfd*). The channel-fill is characterized by rounded boulders (*b*). *Hammer* is 35 cm in length. 1,350 m a.s.l., Hötting Breccia, NCA. **f** Man-made exposure into post-glacial talus fan, strike section. Gravelly to sandy deposits mainly of sheet flows (*sf 1*) are intercalated, along a surface of erosion (*lower dashed line*), by a lense-shaped fill of an ephemerally active torrent channel (*cf 1*). The channel-fill consists of extremely poorly sorted fine gravels to boulders. Channel-fill *cf 1*, in turn, is overlain by a thin interval of sheet flow deposits (*sf 2*) which, in turn, is followed up-section by another torrent channel-fill (*cf 2*). Width of view in lower part of photo is about 9 m. Gravel pit Schönau-Grub, NCA. **g** Breccia deposited from a cohesive debris flow (*df*), sharply overlain (contact indicated by *dashed white line*) by a bouldery openwork breccia to conglobreccia that probably accumulated within an ephemerally active torrent channel (*cf*). Strike section. Width of view is about 3 m. 1,510 m a.s.l., Hötting Breccia, NCA. **h** Detail of filling of ephemerally active torrent channel situated in the distal, low-dipping (10–15°) portion of a lithified talus succession. Note imbricated clast fabric formed by two subrounded cobbles Below the cobbles, larger pores later became filled by sandy to silty sieve deposits (labeled by *arrowtips*, see also Fig. 12a). Pen is 14 cm in length. 1355 m a.s.l., Hötting Breccia, NCA

based on a combination of criteria as listed in Table 3. In particular, unfilled or filled 'underclast pores' can develop only in fluid flows, hence these pore-fills provide a good criterion to distinguish extremely poorly sorted fluid flow rudites from similar debris flow deposits (Fig. 12d).

With respect to the sheet flow deposits, in fully lithified successions, these may be overlooked because they mostly consist of comparatively fine-grained material that, upon cementation, tends to weather in a compact surface. Overall, however, the characteristic 'rhythmic packages' of well-sorted sand and imbricated gravel are readily recognizable (Fig. 12e). Observations on recent talus fans of the NCA indicate that the described sieve lobe deposits originated from overbank deposition of sheet flow during waning floods (Krainer 1988). On the recent talus fans of the Eastern Alps, terraces alongside channels consist mainly of sheet flow deposits. On a few actual talus cones with ephemeral runoff, individual beds and bedsets of this facies were observed with a dip of up to 30° (Fig. 12f).

Rock glacier deposit

An interval interpreted as a rock glacier deposit is present closely south of Innsbruck (location 9 in Appendix supplementary material, see also Fig. 13), between 1,245 and 1,320 m a.s.l (Fig. 12g, h). The interval is at least 60–70 m in thickness; the base is not exposed. It is characterized throughout by an isotropic, extremely poorly sorted, clast-supported fabric of lithic sand to boulders up to about 8 m in size. Most clasts are angular to subangular, but a few subrounded clasts are present. The deposit contains a backweathering matrix of 'chalky' lime mudstone. The matrix content is somewhat variable, and pockets with scarce matrix are locally present. In the matrix, no geopetal lamination was discerned. At about 1,260 m a.s.l., within the rock glacier interval, a lens, up to 7 m in exposed thickness, of better-sorted, distinctly subhorizontally stratified cohesive debris flow breccias is intercalated. Towards the proximal direction (northwest) this lens pinches out, whereas its downslope continuation is covered. The interpreted rock glacier interval is topped by an unconformity with a differentiated relief up to about 15 m in amplitude. The succession directly above the unconformity consists of distinctly better-sorted, gravelly to cobbly openwork breccias of angular to subangular clasts; these breccias are interpreted as rockfall deposits.

Interpretation

The isotropic clast fabric throughout, the extremely poor sorting from sand to boulders, the matrix of chalky lime mudstone, and the localized matrix-poor pockets suggest that the described deposit accumulated from a rock glacier. This interpretation is based on observations in natural and man-made outcrops of rock glaciers that accumulated after the Last Glacial Maximum (LGM). Aside from being unlithified, the post-LGM rock glaciers of the NCA show similar characteristics to the described lithified interval, in particular the presence of a non-laminated matrix of silt- to mud-sized carbonate. Although much of the coarse-clastic fraction of rock glaciers is supplied by rockfalls, the most distinctive differences to rockfall talus facies (as understood herein) include the absence of large volumes of openwork fabric, the apparent absence of geopetally laminated secondary matrix, and the matrix of chalky lime mudstone devoid of sedimentary structures. In the outcrop, the described rock-glacier interval weathers very similar to many outcrops of post-LGM glacial till nourished by local cirque glaciers. As previously mentioned, many talus successions of the NCA shed into glacial cirques that, in many

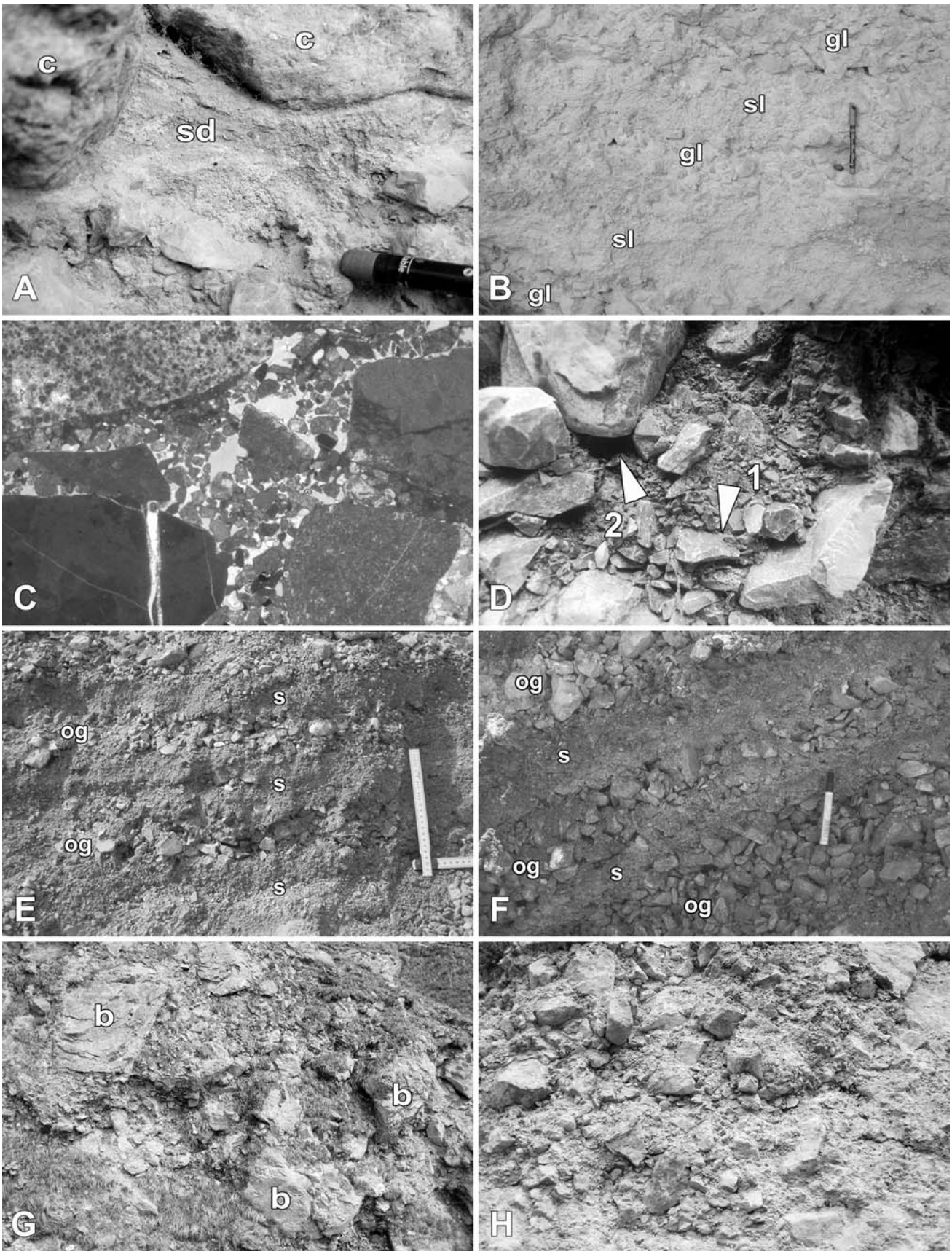
c
c
sd
A
gl
sl
gl
sl
B
gl
C
1
2
D
s
og
s
og
s
E
og
s
og
s
og
F
b
b
b
G
H

◀ **Fig. 12** Facies of carbonate-lithic talus slopes, Eastern Alps. **a** Detail of Fig. 11h. Formerly open pore space below clasts (*c*) became filled by sieve deposits (*sd*) of faintly laminated sand. *Pen tip* is 10 mm in width. **b** Package of sheet flow deposits characterized by rhythmic interbedding of gravelly layers (*gl*) and sandy layers (*sl*), with the latter showing faint lamination subparallel to stratification. *Pen* is 14 cm in length. 1,350 m a.s.l., Hötting Breccia, NCA. **c** Thin-section photomicrograph of gravelly sheet flow deposit. Angular to well-rounded clasts of carbonate rocks, embedded in a matrix of winnowed carbonate-lithic grainstone. Width of view is 17 mm. Parallel nicols. **d** Extremely poorly sorted, sandy to bouldery deposit of an ephemerally active torrent channel on a talus fan. Note pocket of winnowed gravel (*arrowtip 1*), and open pore (*arrowtip 2*) below a small boulder. Width of view is 60 cm. Guggenalm, NCA. **e** Decimeter-scale rhythms composed of openwork layers of poorly to well-sorted, fine to medium gravel (*og*), vertically changing with layers of winnowed, medium to coarse sand (*s*). Such rhythms accumulate from gently lens-shaped sieve lobes during waning flood. *Vertical scale bar* is 22 cm in length. Gravel pit Nagele, NCA. **f** Detail of proximal part of talus cone dominated by fluid flow deposits. Stratification dips with about 30°. Package shown in photo consists of a rhythmic interbedding of openwork gravel (*og*) and carbonate-lithic coarse sand (*s*). *Pen* is 14 cm in length. 2,190 m a.s.l., Oberreintalschrofen, NCA. **g** Detail of an interval interpreted as lithified rock glacier. The deposit is clast-supported, shows an isotropic clast fabric of angular to subangular gravels to boulders (a few labeled *b* in photo) up to about 8 m in size, and contains a matrix of poorly lithified, chalky lime mudstone. Width of view is 7 m. 1,280 m a.s.l., Hötting Breccia, NCA. **h** Detail of same interval as shown in the preceding figure. Note isotropic clast fabric. Width of view is 1.5 m. 1,255 m a.s.l., Hötting Breccia, NCA

cases, contain fossil rock glaciers (see Hera 1997). During deglaciation, the cirques were filled for some time by glaciers that degraded via a rock-glacier stage. It is thus conceivable that some fossil talus successions may be underlain by a rock glacier deposit. An alternative interpretation of the described interval is that it represents amalgamated, extremely poorly sorted cohesive debris flows. Some contribution of debris-flows, upon melting of ice, cannot be definitely ruled out. Throughout the succession of the Hötting Breccia (location 9 in Fig. 1), however, where significant debris-flow deposition had taken place, stratification is present; this is also supported by the intercalated bedded lens of cohesive debris flow breccias within the interpreted rock glacier interval.

Facies associations

Rockfall talus

This facies association is characterized by a prevalence of rockfall breccias, typically in intervals of a few meters to about 100 m in preserved thickness (Fig. 6e, f; Table 4). In all observed cases, rockfall talus as a separate facies association comprises the basal part of a lithified talus succession at site. As mentioned, the basal portions of lithified talus successions with rockfall talus may be situated at different altitudes. A few successions of rockfall talus, such as that of Eibental in Halltal (location 5 in Fig. 1), in their lower part may consist almost entirely of unbedded rockfall breccias. In other successions of rockfall talus, cohesive debris flow breccias are locally intercalated. In addition, faintly stratified lenses a few decimeters to a few meters thick of very poorly to moderately sorted, subangular to subrounded, gravels to cobbles may be

Table 3 Criteria for distinction of ruditic fills of torrential channels (fluid flow deposits) from ruditic debris flow deposits in very proximal, steep-gradient ephemeral alluvial systems (alluvial fans, talus cones), Eastern Alps

	T: Thickness E: Lateral extent in dip/strike Sh: Shape of lithosome	So: Sorting R: Rounding	Imbrication	Matrix	Other features
Debris flow deposits	T: few cm to a few meters E, dip: few meters to >100 m E, strike: few meters to a few 10 s of meters Sh: Non-erosive base, ± planar top	So: extremely poor, lime mud to boulders R: angular to rounded	Downflow-oriented clast imbrication of a(i,p) b(t,p) type	(a) Lime mud, argillaceous-silty lime mud (b) Lime mud to lithic sand	Projecting clasts at bed top Underclast pores absent Pores formed by elutriation and/or dissolution of matrix
Ruditic channel-fills of torrential flows	T: few dm a few meters E, dip: few meters to a few 10 s of meters E, strike: few meters to a few 10 s of meters Sh: Base and top climbing and falling: erosive base, lenticular in dip section	Extremely poor, sand to boulders R: angular to subrounded	Downstream clast imbrication of b(i,p) a(t,p) type	Lithic sand	Underclast pores below 'outsize clasts' Laterally vertically associated and interfingering with sieve lobes and riffles Open primary pore space filled by secondary matrix (silt to lime mud) with geopetal lamination

Figures for thickness, lateral extent, and shape refer to typical examples

Table 4 Facies associations of carbonate-lithic talus slope successions

Facies association	Characteristics	Presence	Locations (examples)	Remarks
Rockfall talus	Thicker successions of rockfall facies devoid of or poor in other facies (debris flows, alluvial talus)	Stratigraphically lowest/oldest part of successions; locally also layers in upper part of talus	Brandjoch-South, Eibental, Gerschrofen (Hötting Breccia), Rossfall (Hötting Breccia), Tawald	Presumably common but rarely exposed
Scree talus	Dominated by grain flow breccias; with intercalated rockfalls and debris flows	Main association of upper part of mature talus slopes	Arzler Reissn (Hötting Breccia), Aspachhütte, Höttinger Reissn-Brandjoch (Hötting Breccia), Steinkarlgrat, Larchetstock, Tawald, Törl, and others	Widespread in proximal part of talus slopes
Debris-flow talus	Dominated by cohesive debris flow rudites; commonly with intercalated alluvial talus and/or scree talus	Prevalent association of talus slopes on rocks that weather under production of abundant carbonate mud	Col Rodella, Duftelalpe, Kleiner Karkopf, Koglkofel, Rossfall, Tawald, and others	Widespread in proximal to distal part of talus slopes May comprise entire talus slopes
Alluvial talus	Dominated by fluid flow rudites; typically with intercalated debris flow talus	(1) Typical for up to about 20–25° steep part of talus cones (talus fans) (2) Within ephemeral runoff chutes up to 30–35° in steepness	(1) Ahornboden, Höttinger Graben (locally), Kleiner Karkopf, Urschenbach (2) Xanderstal	Successions dominated by alluvial talus less common

See Fig. 1 and table in electronic supplementary material for locations

present, and record reworking of rockfall-derived clasts during ephemeral surface runoff. Because the basal part of talus successions in most cases has been eroded or is not exposed, preserved packages of rockfall talus are relatively uncommon. In well-preserved successions, however, the basal rockfall talus is always overlain by other talus facies associations.

Scree talus

The facies association termed scree talus is characterized by grain flow breccias associated with changing but subordinate amounts of cohesive debris flow breccias and/or with rockfall breccias (Figs. 6h, 9c–g; Table 4). Scree talus is characteristic of the medial to apical portion of many lithified talus successions. Seen from a distance, scree talus shows a distinctly bedded appearance and, as a result of the prevalence of grain flow breccias, the bedding typically dips between about 25 and 35°. The grain flow breccias that characterize scree talus are intercalated with layers of cohesive debris flows breccias. The cohesive debris flow breccias may be present in sheet-like to gently lenticular lithosomes commonly about 10–40 cm in thickness, and typically consist of clast-supported, very poorly sorted angular gravels with a matrix of carbonate-lithic packstone to lime mudstone. In the outcrop, the cohesive debris flows breccias tend to weather out. As described, the fossil talus slopes also contain a few intervals up to a few meters thick of extremely poorly sorted, cobbly to bouldery, breccias that accumulated from debris flows and/or rockfalls. Successions of lithified scree talus are common, and may be hundreds of meters in downslope extent and tens of meters to about 100 m in thickness.

Debris flow talus

This facies association is characterized by cohesive debris flow breccias, in a proportion of about 1/1 to >1/1 over other talus facies (Fig. 11a, b). Other facies commonly associated with debris flow talus, in highly variable relative amounts, include grain flow breccias, torrent breccias to conglobreccias, and rockfall breccias. Debris flow talus was observed from the low-dipping, distal to steep-dipping, apical portions of lithified talus successions. Consequently, the dip of successions of debris flow talus ranges between a few degrees to about 30°. In debris flow talus, the cohesive debris flow breccias most commonly are clast-supported. Beds supported by a matrix of carbonate-lithic mud are rare.

Alluvial talus

This facies association designates talus successions, or portions thereof, with a prevalence of torrent rudites over

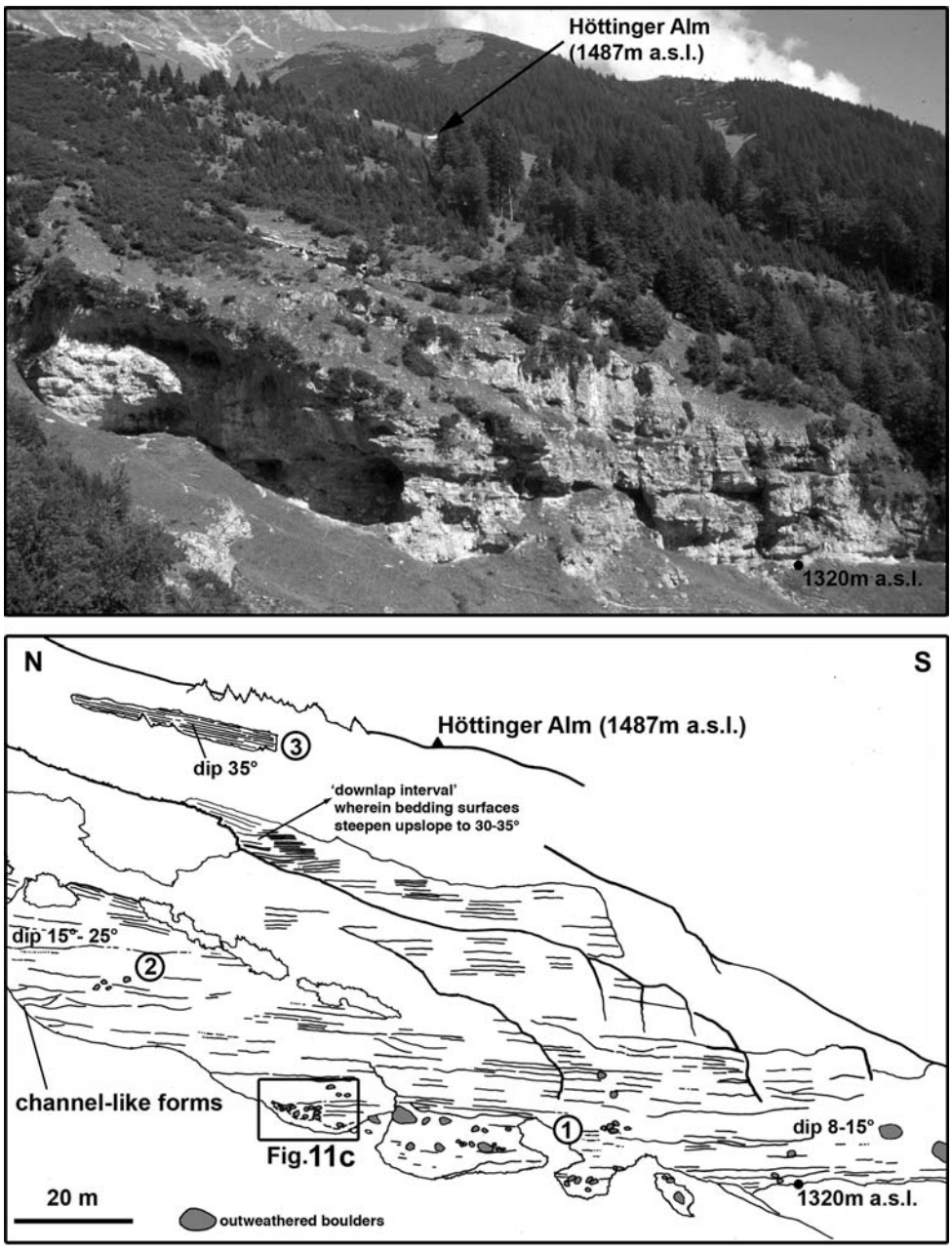

Fig. 13 Outcrop in Höttinger Graben near Innsbruck (location number 9 in Fig. 1). The lower part of the outcrop (*interval labeled 1*) consists of a package of beds that dip with 8–15°. This package consists mainly of moderately sorted to extremely poorly sorted, gravelly to bouldery breccias and conglobreccias that accumulated from ephemeral surface runoff, in the distal part of an immature talus slope. Above (*interval labeled 2*), bedding dip steepens to between about 15–25°, within an indistinctly bedded package with downward-convex, 'channel-like' stratification surfaces. This package, in turn, is overlain and downlapped by a succession (*labeled 3*) mainly of well-bedded, moderately to well-sorted medium to coarse-grained openwork breccias that dip with 30–35°, and that accumulated from grain flows on a mature talus slope. Package number 3 extends up to 1,700–1,900 m a.s.l., where it onlaps onto rock cliffs. 20-m scale is valid for foreground

other facies (Figs. 11c–h, 12a–f). In the same outcrop, alluvial talus may be vertically and/or laterally associated with debris flow talus (Fig. 13). The typical dip of packages of alluvial talus ranges from a few degrees up to about 15°. On talus cones, individual beds and bedsets of sheet flow breccias may dip with up to 30°. Because of repeated cut-and-fill of channels and associated terraces and sieve lobes, and because of intermittent deposition of other talus facies (e.g., cohesive debris flows), successions of alluvial talus consist of a complicated meter-scale facies mosaic. Alluvial talus was observed in two positions, (a) in the distal, low-dipping portions of mature talus slopes, and (b) in the lower part of thicker talus successions, where it formed during an early, immature stage of talus development.

Depositional geometries

The accumulation pattern illustrated in Fig. 2b implies that talus slope development is accompanied not only by a change in prevalent facies but also shows characteristic depositional geometries. Along the toe of mountain flanks, the truncation surface on top of the bedrock is characterized by a differentiated relief on a scale of meters to hundreds of meters (Fig. 14). We assume that this relief is

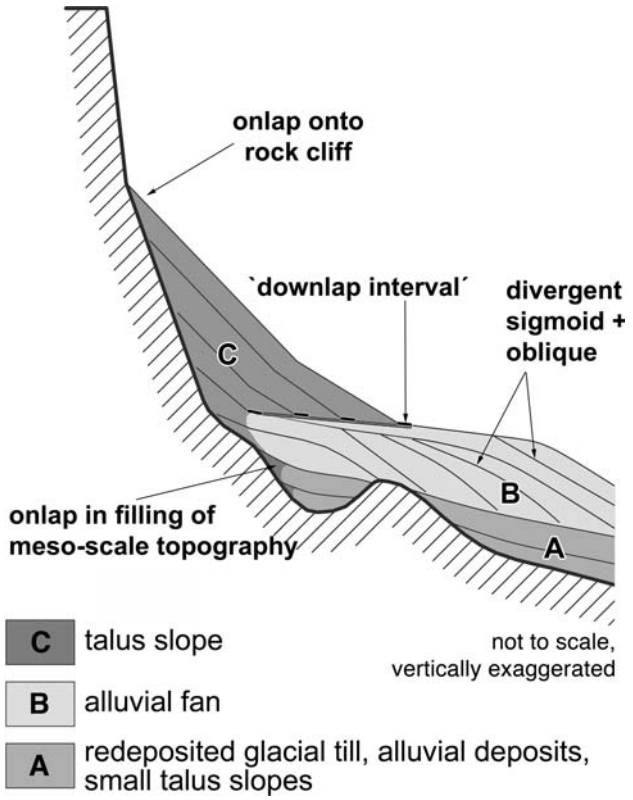

Fig. 14 Schematic summary of depositional geometries in alluvial fan-to-talus slope successions. **a** In areas with a differentiated meso-scale relief (probably largely of sub-glacial origin), local onlap of hillslope colluvium and infill by colluvial to alluvial deposits takes place. **b** In alluvial fan successions, divergent-sigmoidal and divergent-oblique depositional geometries are common, and result from phases of aggradation and progradation of the fan. **c** Up-section, along the mountain flank, the alluvial fan is overlain by talus slopes. At their downslope termination, the talus slopes pinch out and downlap onto the alluvial fan succession within a narrow stratigraphic interval ('downlap interval')

mainly produced by subglacial erosion during pleniglacials. During and after deglaciation, local morphological depressions of the truncation surface become first filled by alluvial fan deposits, hillslope colluvium, and small talus accumulations (phase A in Fig. 14). Above, in alluvial fan packages that may provide the foundation to overlying, younger talus slopes, sigmoids and obliques are common (phase B in Fig. 14, see also Fig. 15c, d). Oblique stratal patterns result from progradation of the depositional front of an alluvial fan, downslope of the intersection point, by combined sheet flow-sieve lobe deposition, while the channel remains close to local intermittent base-level (= top of obliques) (Fig. 15a–d). A sigmoid or sigmoid-divergent pattern results from combined aggradation-progradation of a fan. The onlap mainly of the upper, steep-dipping part of lithified talus slopes onto rock cliffs is exposed at many locations (phase C in Fig. 14; Ampferer 1907; Penck 1921).

The most significant depositional geometry is represented by a stratigraphic interval in which bedding surfaces markedly steepen over a short lateral/vertical distance (labeled 'downlap interval' in Fig. 14; see also Figs. 13, 15e, f). This interval has been recognized at several locations (Figs. 13–15). Because of its similarity to a downlap 'surface' as identifiable with the vertical resolution of reflection seismic sections of marine depositional sequences (Van Wagoner et al. 1988), and because it is not strictly a surface but an interval, it is termed 'downlap interval' herein. The downlap interval records the overall change from accumulation of a low-dipping slope-front fill (alluvial fans to talus fans) to buildup and progradation of steeper-dipping (25–35°) large talus slopes. Because the development of the downlap interval is related to the concept of talus maturity, depending on the ratio of cliff height to talus height, it is clear that some of the presently active talus accumulations are still in an early, immature stage, while others have already attained a mature stage. On the surface of active talus slope-alluvial fan systems, the break in slope from the lower-dipping surface of the fan to the steeper surface of the talus upslope can be considered as a 'snapshot' of downlap in formation.

Synthesis: facies architecture of Quaternary carbonate-lithic talus successions

The described observations are combined to a generalized concept of talus development (Fig. 16). During Pleistocene glaciations, rocky valley flanks became steepened by glacial erosion. Immediately after deglaciation, rapid redeposition of glacial till takes place initially. During glacial retreat, in many cirques, rock glaciers form which later become fossil. Stripping of glacial ice, from oversteepened valley flanks and cliffs up to more than 1,000–1,500 m in relief, initially leads to the formation of low-dipping talus dominated by rockfall deposits. With progressive buildup and onlap of talus slopes onto retreating cliffs, the talus surface steepens while the relief amplitude of cliffs and mean energy of rockfalls decrease. As a result, a progressive change of prevalent processes of deposition and redeposition takes place. Because of the steepened and longer slope surface, cohesive debris flows and deposition from fluid flows become more important than deposition from rockfalls. Under a cliff still high enough to focus larger amounts of surface runoff, redeposition of rockfall-derived material by ephemeral surface runoff and/or by cohesive debris flows becomes important. Whether deposition from fluid flows or from cohesive debris flows prevails is largely controlled by the geology of the host rocks and the shape of the cliff (see above). Under cliffs that weather under production of abundant sand-sized

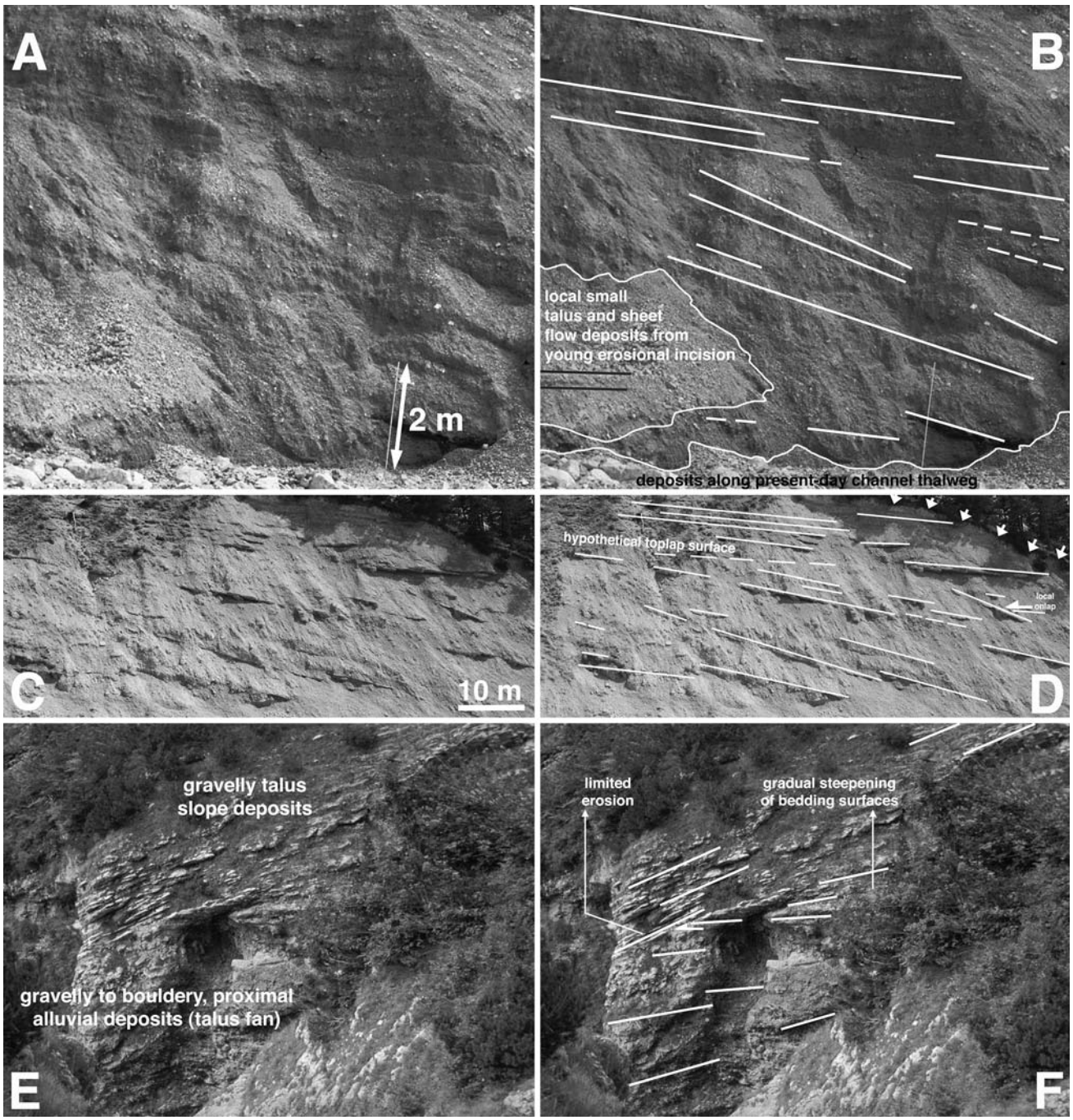

Fig. 15 Depositional geometries of alluvial fans and talus successions. **a**, **b** Outcrop of erosionally incised stream-dominated talus fan (Guggenalm, NCA). The interval shown consists of stacked sheet flow deposits of gravel to coarse sand composition. A lower, steeper-dipping package is separated along a surface of minor erosion (similar to a 'toplap surface' in sequence stratigraphy) from an overlying, lower-dipping package. This is a common depositional geometry in talus cones and alluvial fans. **c**, **d** Stratal packages in a partly lithified alluvial fan succession (Urschenbach, NCA). A lower, steeper-dipping package mainly of gravelly sheet-flow deposits is vertically separated along an interpreted toplap surface from an overlying, lower-dipping package again of gravelly sheet-flow deposits. The vegetated top of the alluvial fan is marked by *white arrows*. **e**, **f** Outcrop at 1,120 m a.s.l., in a lithified alluvial fan-to-talus succession (Hötting Breccia, NCA). The lower part of the outcrop consists of low-dipping, very thick-bedded, extremely poorly sorted breccias to conglobreccias deposited mainly from torrential floods and from debris flows. This lower package can be mapped down-valley over a distance of about 1.2 km. The better-stratified deposits in the upper part consist of talus slope breccias deposited mainly from grain flows and from cohesive debris flows. In the upper package, beds dip with 25–30°. The talus slope breccias downlap and overlie the fan deposits along a surface of minor erosion or along a narrow stratigraphic interval in which bedding surfaces markedly steepen upslope. The package of talus-slope breccias represents the lowest part of a mappable succession of lithified talus slopes that here are preserved up to about 1,600 m a.s.l. Width of view is about 40 m

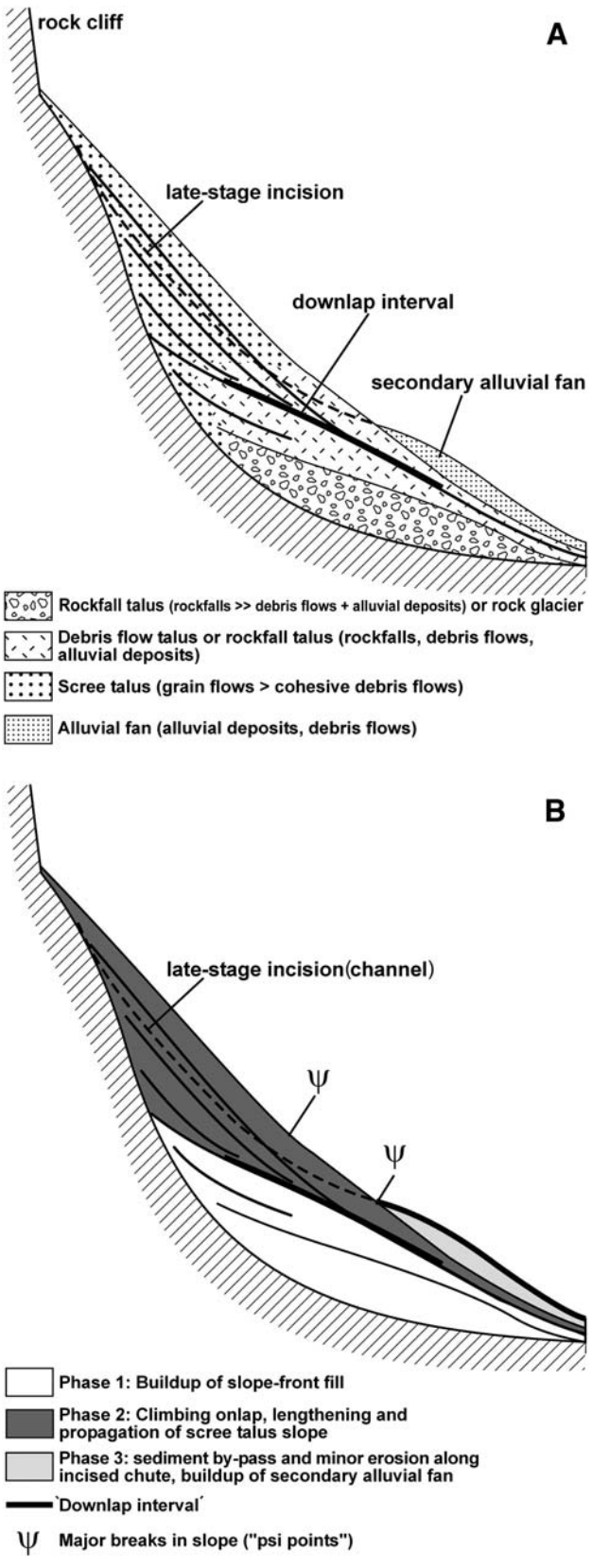

Fig. 16 Scheme of facies architecture and depositional phases of carbonate-lithic talus slopes, Eastern Alps. **a** Facies architecture and depositional geometry. The most notable features are (1) the progressive steepening of the talus slope surface in time, leading to and accompanied by a change of prevalent depositional processes and facies, until a stable mature state is reached, (2) the presence of a downlap interval corresponding to the time when the proximal, 30–35° steep part of the talus slope had developed and prograded over the slope-front fill of older deposits, and (3) late-stage incision along channels and development of secondary alluvial fans farther down slope. **b** Main depositional phases during formation of a mature talus slope. Phase 1: Development of a comparatively low-dipping slope-front fill along the lower part of the cliff. Phase 2: Rapidly climbing onlap of talus, lengthening of talus slopes and progradation over underlying deposits along a downlap interval. Phase 3: Late-stage incision and development of secondary alluvial fan farther down slope (as shown), or direct debouch or incised channel into stream (not shown in figure)

material and carbonate mud, the slope may continue to form as a debris-flow dominated talus.

In contrast, in successions that tend to weather more by production of discrete clasts of gravel to cobble size, a threshold is attained whereby the talus succession itself can accommodate large amounts of water, such that processes of surface runoff decrease in importance. At this state, the talus becomes dominated by grain-flow deposition and particle creep, i.e., it changes from a former alluvial/debris-flow talus to a scree talus. This change is associated with a steepening of the talus depositional surface and downlap onto the underlying succession (Fig. 14). In this mature stage, rockfalls can run out over a longer distance and segregate for different clast sizes, leading to size-grading of rockfall-derived grains along the talus slope (cf. Fig. 2b). The grain segregation of rockfalls, in turn, is the cause for the openwork clastic fabric in the proximal part of many talus slopes, and for grain flows and particle creep. Finally, under persistence of interglacial climatic conditions, the delivery of clastic sediment from cliffs progressively buried by talus slopes progressively decreases (cf. Fig. 2). In addition, upon interglacial climatic warming, depending on the altitude of a considered location, the wet-periglacial climatic window favourable for effective talus production may shift still higher up. As a result of combined cliff burial and climatic warming, talus activity lowers, and the slope becomes vegetated and/or is incised by channels. In this late stage, secondary alluvial fans may develop down slope from channels incised into the talus slope.

Discussion

Previous authors had speculated on the palaeoclimatic significance of Eastern-Alpine lithified talus relicts

(Ampferer 1907; Penck 1921; Wehrli 1928; Cornelius 1941; Paschinger 1950), with conflicting results. The crucial problem in palaeoclimatic interpretation of talus successions is that they develop under sensitive feedbacks between cliff degradation, cliff shape and height, lithology, tectonic deformation, talus accumulation, microclimate, and regional climate. The prime difficulty is then to unequivocally distinguish changes in talus facies induced by (micro-)climate from changes induced by the depositional system itself. The ambiguity in palaeoclimatic interpretation of fossil talus successions is underscored by the marked differences in depositional processes and deposits on the surface of presently active talus slopes over short lateral distances (see above). Thus, aside from marked climatic changes such as glacial-interglacial cycles, the recognition of shorter-term and more subtle changes in climate from talus successions is risky (see also Van Steijn et al. 1995; Hétu and Gray 2000). In addition, because the largest volume of talus slopes accumulates in a short time interval after deglaciation at a site, followed by a longer period of lower activity and/or vegetation and erosion, the capacity of talus slopes to faithfully record minor climatic changes in time is inherently limited. By analogy to a well-preserved talus-to-alluvial fan succession of Riss-Würm interglacial age (Hötting Breccia, location number 9 in Fig. 1), it was often assumed that at least most lithified talus relicts of the Eastern Alps accumulated and lithified during the Eemian. In contrast, our U/Th age data of cements imply that lithified talus successions had accumulated and lithified at markedly different times during the Quaternary.

Conclusions

1. Integrated observations from recent talus slopes and from lithified Quaternary talus relicts (Eastern Alps, Austria) indicate an overall predictable relation between talus slope maturity, depositional geometry, and sedimentary facies.
2. After exposure of cliffs by deglaciation or rocksliding, a low-dipping immature rockfall talus or (in case of deglaciation and position in appropriate setting) a rock glacier initially accumulates. Upon progressive buildup and steepening of the proximal segment of the talus slope, prevalent processes of deposition change to grain flows and 'sorted rockfall deposition' in the proximal steep-dipping (30–35°) slope segment, while deposits of debris flows, ephemeral fluid flows, and rare large rockfalls prevail on the distal, lower-dipping segment of slope. In mature talus slopes, the proximal steep-dipping slope succession overlies the lower-dipping deposits of the distal slope along a narrow 'downlap interval'.
3. Accumulation rates of Eastern Alpine carbonate-rocky talus slopes are variable over time, and vary highly among different slopes. Immediately after cliff exposure by deglaciation or rocksliding, talus can aggrade at rates of up to a few tens of meters per 1,000 years, but initially high accumulation rates decrease rapidly upon buildup and maturation of slope.
4. On the present carbonate-lithic talus slopes of the Eastern Alps the processes of sediment delivery, sediment transport, final deposition and deposit overprint in many cases change over lateral distances of tens to a few hundreds of meters. This gives rise to different types of talus slopes that nevertheless accumulate under the same climate.
5. The facies, facies architecture, and depositional geometry of talus successions mainly result from dynamic feedbacks between: (a) bedrock geology, initial cliff height, and talus accumulation ('internal control'), and probably (b) the rate and amplitude of climatic changes at a site ('external control'). In vertical sections of talus slope successions, at present it appears difficult to clearly distinguish effects of minor climatic changes from feedbacks resulting from the progressive change of a cliff-talus ensemble.

Acknowledgements Financial support from project 16114-NO6 "Quaternary talus, Northern Calcareous Alps" of the Austrian Research Foundation (to D. S.) is gratefully acknowledged. Robert Scott, Precision Stratigraphy Associates (Cleveland, US) and an anonymous referee are thanked for helpful reviews. Discussions with Hanns Kerschner and Georg Kaser, Institute of Geography, with Gernot Patzelt, former Institute of Alpine Research, and with Karl Krainer, Institute of Geology and Palaeontology, all University of Innsbruck, provided important input. Field trips with Alfred Gruber, Geological Survey of Austria (Vienna), with Christoph Prager, alpS Center for Natural Hazard Management (Innsbruck), and Ulrich Haas, Bayerisches Geologisches Landesamt (Munich), aided to shape concepts expressed herein. Reviews of an earlier version of the manuscript by Karl Krainer (Innsbruck), Dirk van Husen (Altmünster) and Andreas von Poschinger (München) are acknowledged. Helena Rodnight, Institute of Geology, University of Innsbruck, is thanked for correcting the English.

References

Akerman HJ (1984) Notes on talus morphology and processes in Spitsbergen. Geogr Ann 66A:267–284. doi:10.2307/520850

Allen JRL (1970) The avalanching of granular solids on dune and similar slopes. J Geol 78:326–351

Allen PA (1997) Earth surface processes. Blackwell Science, Oxford, p 404

Ampferer O (1907) Über Gehängebreccien der nördlichen Kalkalpen. Jahrb geol Reichsanst 57:727–752

André M-F (1997) Holocene rockwall retreat in Svalbard: a triple-rate evolution. Earth Surf Process Landf 22:423–440 10.1002/(SICI)1096-9837(199705)22:5<423::AID-ESP706>3.0.CO;2-6
Bakker JP, Le Heux JWN (1952) A remarkable new geomorphological law. Proc Koninkl Akad Wetenschappen 55(399–410):554–571
Ballantyne CK (2002) Paraglacial geomorphology. Quat Sci Rev 21:1935–2017. doi:10.1016/S0277-3791(02)00005-7
Bates RL, Jackson JA (eds) 1980 Glossary of geology. American Geological Institute, Falls Church (Va), 749 pp
Bertran P, Texier J-P (1994) Structures sédimentaires d'un cone de flots de débris (Vars, Alpes francaises méridionales). Permafr Periglac Proc 5:155–170. doi:10.1002/ppp.3430050305
Bertran P, Coutard J-P, Ozouf J-C, Texier J-P (1995) Dépots de pente calcaires du nord de l'Aquitaine. Répartition stratigraphique et géographique de faciès. Z Geomorph N F 39:29–54
Bones JG (1973) Process and sediment size arrangement on high arctic talus, southwest Devon Island, N. W. T., Canada. Arct Alp Res 5:29–40. doi:10.2307/1550297
Brückl E, Brunner FK, Gerber E, Scheidegger AE (1974) Morphometrie einer Schutthalde. Mitt österr geogr Ges Wien 116:79–96
Caine N (1969) A model for alpine talus development by slush avalanching. J Geol 77:92–100
Chandler RJ (1973) The inclination of talus, Arctic talus terraces, and other slopes composed of granular materials. J Geol 81:1–14
Chorley RJ (2000) Classics in physical geography revisited: Mackin JH (1948) concept of the graded river (Geol Soc Am Bull 59: 463–511). Prog Phys Geogr 24:563–578
Church M, Stock RF, Ryder JM (1979) Contemporary sedimentary environments on Baffin Island, N. W. T., Canada: debris slope accumulations. Arct Alp Res 11:371–402. doi:10.2307/1550559
Clowes A, Comfort P (1987) Process and landform: an outline of contemporary geomorphology. Oliver and Boyd, Edinburgh, p 335
Collinson JD, Thompson DB (1989) Sedimentary structures. Unwin Hyman, London, p 207
Coltorti M, Dramis F (1995) The chronology of upper Pleistocene stratified slope-waste deposits in central Italy. Permafr Perigl Process 6:235–242. doi:10.1002/ppp.3430060304
Cornelius HP (1941) Über die Bedingtheit der interglazialen Schuttumhüllung der Alpen. Ber Reichsst Bodenforschung 1941:169–179
Cruden DM, Hu X-Q (1999) The shapes of some mountain peaks in the Canadian Rockies. Earth Surf Process Landf 24: 1229–1241 10.1002/(SICI)1096-9837(199912)24:13<1229::AID-ESP42>3.0.CO;2-1
Fliri F, Bortenschlager S, Felber H, Heissel W, Hilscher H, Resch W (1970) Der Bänderton von Baumkirchen (Inntal, Tirol). Eine neue Schlüsselstelle zur Kenntnis der Würm-Vereisung der Alpen. Z Gletsch kd Glazialgeol 6:5–35
Francou B, Manté C (1990) Analysis of the segmentation in the profile of Alpine talus slopes. Permafr Perigl Process 1:53–60. doi:10.1002/ppp.3430010107
Frisch W, Székely B, Kuhlemann J, Dunkl I (2000) Geomorphological evolution of the Eastern Alps in response to Miocene tectonics. Z Geomorph N F 44:103–138
Frisch W, Kuhlemann J, Dunkl I, Székely B (2001) The Dachstein paleosurface and the Augenstein Formation in the Northern Calcareous Alps—a mosaic stone in the geomorphological evolution of the Eastern Alps. Int J Earth Sci 90:500–518. doi:10.1007/s005310000189
Gardner J (1970) Geomorphic significance of avalanches in the Lake Louise area, Alberta, Canada. Arct Alp Res 2:135–144. doi:10.2307/1550348
Gardner J (1971) Morphology and sediment characteristic of mountain debris slopes in Lake Louise District (Canadian Rockies). Z Geomorph N F 15:390–403
Gardner JS (1979) The movement of material on debris slopes in the Canadian Rocky Mountains. Z Geomorph N F 23:45–57
Gerber EK (1969) Bildung von Gratgipfeln und Felswänden in den Alpen. Z Geomorphol Suppl 8:94–118
Hales TC, Roering JJ (2005) Climate-controlled variations in scree production, Southern Alps, New Zealand. Geology 33:701–704. doi:10.1130/G21528.1
Hampton MA (1979) Buoyancy in debris flows. J Sediment Petrol 49:753–758
Hera U (1997) Gletscherschwankungen in den Nördlichen Kalkalpen seit dem 19. Jahrhundert. Münchener geogr Abh B25:1–205
Hétu B, Gray JT (2000) Effects of environmental change on scree slope development throughout the postglacial period in the Chic-Choc Mountains in the northern Gaspé Peninsula, Québec. Geomorphology 32:335–355. doi:10.1016/S0169-555X(99)00103-8
Hutchinson JN (1998) A small-scale field check on the Fisher-Lehmann and Bakker-Le Heux cliff degradation models. Earth Surf Process Landf 23:913–926. doi:10.1002/(SICI)1096-9837(199810)23:10<913::AID-ESP911>3.0.CO;2-G
Jomelli V, Bertran P (2001) Wet snow avalanche deposits in the French Alps: structure and sedimentology. Geogr Ann 83A:15–28. doi:10.1111/1468-0459.00141
Jomelli V, Francou B (2000) Comparing the characteristics of rockfall talus and snow avalanche landforms in an Alpine environment using a new methodological approach: Massif des Ecrins, French Alps. Geomorphology 35:181–192. doi:10.1016/S0169-555X(00)00035-0
Kirkby MJ, Statham I (1975) Surface stone movement and scree formation. J Geol 83:349–362
Kotarba A, Strömquist L (1984) Transport, sorting and deposition processes of Alpine debris slope deposits in the Polish Tatra Mountains. Geogr Ann 66A:285–294. doi:10.2307/520851
Krainer K (1988) Sieve deposition on a small modern alluvial fan in the Lechtal Alps (Tyrol, Austria). Z Geomorph N F 32:289–298
Linzer H-G, Ratschbacher L, Frisch W (1995) Transpressional collision structures in the upper crust: the fold-thrust belt of the Northern Calcareous Alps. In: Neubauer F, Wallbrecher E (eds) Tectonics of the Alpine-Carpathian-Pannonian Region. Tectonophysics 242:41–61
Luckman BH (1976) Rockfalls and rockfall inventory data: some observations from the Surprise Valley, Jasper National Park, Canada. Earth Surf Processes 1:287–298. doi:10.1002/esp.3290010309
Luckman BH (1977) The geomorphic activity of snow avalanches. Geogr Ann 59A:31–48. doi:10.2307/520580
McCarroll D, Shakesby RA, Matthews JA (2001) Enhanced rockfall activity during the Little Ice Age: further lichenometric evidence from a Norwegian talus. Permafr Perigl Process 12:157–164. doi:10.1002/ppp.359
Montgomery DR, Buffington JM (1997) Channel-reach morphology in mountain drainage basins. Geol Soc Am Bull 109:596–611 10.1130/0016-7606(1997)109<0596:CRMIMD>2.3.CO;2
Morris PH, Williams DJ (1999) Worldwide correlations for subaerial aqueous flows with exponential longitudinal gradients. Earth Surf Process Landf 24:867–879 10.1002/(SICI)1096-9837(199909)24:10<867::AID-ESP16>3.0.CO;2-L
Nieuwenhuijzen ME, van Steijn H (1990) Alpine debris flows and their sedimentary properties. A case study from the French Alps. Permafr Perigl Proc 1:111–128. doi:10.1002/ppp.3430010204
Obanawa H, Matsukura Y (2006) Mathematical modeling of talus development. Comput Geosci 32:1461–1478. doi:10.1016/j.cageo.2006.05.004
Ostermann M (2006) Thorium-uranium age-dating of "impure" carbonate cements of selected Quaternary depositional systems of western Austria: results, implications, problems. Unpubl PhD Thesis, University of Innsbruck, 173 pp

Ostermann M, Sanders D, Kramers J (2006) $^{230}Th/^{234}U$ ages of calcite cements of the proglacial valley fills of Gamperdona and Bürs (Riss ice age, Vorarlberg, Austria): geological implications. Aust J Earth Sci 99:31–41

Ostermann M, Sanders D, Prager C, Kramers J (2007) Aragonite and calcite cementation in 'boulder-controlled' meteoric environments on the Fern Pass rockslide (Austria): implications for radiometric age-dating of catastrophic mass movements. Facies 53:189–208. doi:10.1007/s10347-006-0098-5

Otto JC, Sass O (2006) Comparing geophysical methods for talus slope investigations in the Turtmann valley (Swiss Alps). Geomorphology 76:257–272. doi:10.1016/j.geomorph.2005.11.008

Paschinger H (1950) Morphologische Ergebnisse einer Analyse der Höttinger Brekzie bei Innsbruck. Schlern-Schriften 75:7–86

Patzelt G, Poscher G (1993) Bemerkenswerte geologische und quartärgeologische Punkte im Oberinntal und im äusseren Ötztal. Arbeitstagung Geol Bundesanst, Geologie des Oberinntaler Raumes, pp 205–216

Penck A (1921) Die Höttinger Breccie und die Inntalterrasse nördlich Innsbruck. Abh preuss Akad Wiss, phys-math Kl 1920:1–136

Penck W (1924) Die morphologische Analyse. Ein Kapitel der physikalischen Geologie. Verlag J Engelhorns Nachfolger, Stuttgart, 284 pp

Pérez FL (1989) Talus fabric and particle morphology on Lassen Peak, California. Geogr Ann 71A:43–57. doi:10.2307/521007

Pitman WC III, Golovchenko X (1983) The effect of sealevel change on the shelfedge and slope of passive margins. In: Stanley DJ, Moore GT (eds) The shelfbreak: critical interface on continental margins, vol 33. Soc Econ Pal Min Spec Publ, pp 41–58

Prager C, Zangerl C, Brandner R, Patzelt G (2007) Increased rockslide activity in the Middle Holocene? New evidences from the Tyrolean Alps (Austria). In: McInnes R, Jakeways J, Fairbank H, Mathie E (eds) Landslides and climate change, challenges and solutions. Taylor and Francis, London, pp 25–34

Prick A (1997) Critical degree of saturation as a threshold moisture level in frost weathering of limestones. Permafr Perigl Process 8:91–99 10.1002/(SICI)1099-1530(199701)8:1<91::AID-PPP238>3.0.CO;2-4

Rapp A (1960) Recent development of mountain slopes in Kärkevagge and surroundings, Northern Scandinavia. Geogr Ann 42:65–200. doi:10.2307/520126

Rodine JD, Johnson AM (1976) The ability of debris, heavily freighted with coarse clastic materials, to flow on gentle slopes. Sedimentology 23:213–234. doi:10.1111/j.1365-3091.1976.tb00047.x

Sanders D, Ostermann M (2006) Depositional setting of the sedimentary rocks containing the "warm-interglacial" fossil flora of the Höttinger Brekzie (Pleistocene, Northern Calcareous Alps, Austria): a reconstruction. Veroffentlichungen Tiroler Landesmuseums Ferdinandeum 86:91–118

Sass O (2006) Determination of the internal structure of alpine talus deposits using different geophysical methods (Lechtaler Alps, Austria). Geomorphology 80:45–58. doi:10.1016/j.geomorph.2005.09.006

Sass O, Wollny K (2001) Investigations regarding Alpine talus slopes using ground-penetrating radar (GPR) in the Bavarian Alps, Germany. Earth Surf Process Landf 26:1071–1086. doi:10.1002/esp.254

Schmid SM, Fügenschuh B, Kissling E, Schuster R (2004) Tectonic map and overall architecture of the Alpine orogen. Eclogae Geol Helv 97:93–117. doi:10.1007/s00015-004-1113-x

Schrott L, Hufschmidt G, Hankammer M, Hoffmann T, Dikau R (2004) Spatial distribution of sediment storage types and quantification of valley fill deposits in an alpine basin, Reintal, Bavarian Alps, Germany. Geomorphology 55:45–63. doi:10.1016/S0169-555X(03)00131-4

Selby MJ (1985) Earth's changing surface. An introduction to geomorphology. Clarendon Press, Oxford, 607 pp

Statham I (1976) A scree slope rockfall model. Earth Surf Processes 1:43–62. doi:10.1002/esp.3290010106

Summerfield MA (1991) Global geomorphology. Longman Scientific and Technical, Essex, 537 pp

Theakstone WH (1982) Sediment fans and sediment flows generated by snowmelt: observations at Austerdalsisen, Norway. J Geol 90:583–588

Van Husen D (1981) Geologisch-sedimentologische Aspekte im Quartär von Österreich. Mitt österr geol Ges 74(75):197–230

Van Husen D (1983a) A model of valley bottom sedimentation during climatic changes in a humid alpine environment. In: Evenson EB, Schlüchter C, Rabassa J (eds) Tills and related deposits. Balkema, Rotterdam, pp 341–344

Van Husen D (1983b) General sediment development in relation to the climatic changes during Würm in the eastern Alps. In: Evenson EB, Schlüchter C, Rabassa J (eds) Tills and related deposits. Balkema, Rotterdam, pp 345–349

Van Husen D (1999) Geological processes during the Quaternary. Mitt österr geol Ges 92:135–156

Van Steijn H (1988) Debris flows involved in the development of Pleistocene stratified slope deposits. Z Geomorph N F Suppl 71:45–58

Van Steijn H, Bertran P, Francou B, Hétu B, Texier J-P (1995) Models for the genetic and environmental interpretation of stratified slope deposits. Permafr Perigl Process 6:125–146. doi:10.1002/ppp.3430060210 Review

Van Wagoner JC, Posamentier HW, Mitchum RM, Vail PR, Sarg RF, Loutit TS, Hardenbol J (1988) An overview of the fundamentals of sequence stratigraphy and key definitions. In: Wilgus CK, Hastings BS, Ross CA, Posamentier H, Kendall CGStC (eds) Sea-level changes—an integrated approach. vol 42. Soc Econ Pal Min Spec Publ, pp 39–45

Wehrli H (1928) Monographie der interglazialen Ablagerungen im Bereich der nördlichen Ostalpen zwischen Rhein und Salzach. Jb Geol Bundesanst 78:357–495

White SE (1981) Alpine mass movement forms (noncatastrophic): classification, description, and significance. Arct Alp Res 13:127–137. doi:10.2307/1551190

Whitehouse IE, McSaveney MJ (1983) Diachronous talus surfaces in the Southern Alps, New Zealand, and their implications to talus accumulation. Arct Alp Res 15:53–64. doi:10.2307/1550981